Design, Synthesis, and Evaluation of *N*-Acyl Modified Sialic Acids as Inhibitors of Adenoviruses Causing Epidemic Keratoconjunctivitis†

Susanne Johansson,‡ Emma Nilsson,§ Weixing Qian,‡ Delphine Guilligay,|| Thibaut Crepin,|| Stephen Cusack,|| Niklas Arnberg,§ and Mikael Elofsson*,‡

Department of Chemistry, Umeå University, SE-901 87 Umeå, Sweden, Department of Clinical Microbiology, Division of Virology, Umeå University, SE-901 87 Umeå, Sweden, and European Molecular Biology Laboratory, EMBL Grenoble, BP 181, 6 Rue Jules Horowitz, 38042 Grenoble Cedex 9, France

Received December 19, 2008

The adenovirus serotype Ad37 binds to and infects human corneal epithelial (HCE) cells through attachment to cellular glycoproteins carrying terminal sialic acids. By use of the crystallographic structure of the sialic acid-interacting domain of the Ad37 fiber protein in complex with sialyllactose, a set of *N*-acyl modified sialic acids were designed to improve binding affinity through increased hydrophobic interactions. These *N*-acyl modified sialic acids and their corresponding multivalent human serum albumin (HSA) conjugates were synthesized and tested in Ad37 cell binding and cell infectivity assays. Compounds bearing small substituents were as effective inhibitors as sialic acid. X-ray crystallography and overlays with the Ad37−sialyllactose complex showed that the *N*-acyl modified sialic acids were positioned in the same orientation as sialic acid. Their multivalent counterparts achieved a strong multivalency effect and were more effective to prevent infection than the monomers. Unfortunately, they were less active as inhibitors than multivalent sialic acid.

Introduction

Despite 50 years of research, the development of antiviral drugs is far behind the development of antibacterial agents. Viruses are obligate intracellular parasites; they are totally dependent on the cellular mechanisms of their host and are thereby difficult to selectively target without disturbing some of the essential functions of the host cell.[1,2] Today, most antiviral drugs on the market target the synthesis of new viral components by deactivating viral enzymes. The need for new antiviral drugs is growing rapidly as more virus diseases are recognized.[3] During the past decade, nonenzymatic processes of the virus life cycle such as attachment to host cells and fusion to and/or penetration through the cell membrane have come into focus for research aimed at development of new antiviral agents.[4] Cell surface oligosaccharides are crucial for the attachment of microbes to and infection of host cells. Despite this central role of oligosaccharides, there are relatively few carbohydrate-based therapeutic agents. The reasons for this are their low absorption after oral administration and sensitivity to metabolic breakdown, leading to poor oral bioavailability and rapid clearance. Another drawback is the weak, often millimolar affinity between monovalent carbohydrates and proteins. Nature overcomes this problem elegantly and improves the binding affinity enormously by gathering carbohydrate conjugates closely together to produce multivalent binding epitopes that simultaneously associate with multiple protein receptors on the attaching cell or organism. This multivalency phenomenon has been extensively discussed and reviewed.[5−7] Since viruses in general attach to host cells in a multivalent manner, one strategy for finding new antiviral drugs might be to target virus adhesion by using antiviral agents that are themselves multivalent.

Our aim was to find antivirals that target adhesion of adenoviruses of types Ad8, Ad19, and Ad37 to human corneal epithelial (HCE[a]) cells. These viruses are the causative agents of the severe ocular condition epidemic keratoconjuctivitis (EKC).[8,9] At present, there are no licensed antiviral agents for treatment of this disease. The viruses are transferred by contact, such as via towels, handshakes, and contaminated tonometers at ophthalmic departments. Thus, these infections are most common in densely populated areas, predominantly in Asia but also in North America and Europe.[10−12] For example, between half a million and one million individuals fall ill from EKC every year in Japan alone.[13] As a result of the infection, the patient is handicapped for weeks, resulting in substantial suffering and economic losses. In some cases the infection leads to permanent impairment of sight.[8]

Adenoviruses interact with their cellular receptors through the fiber proteins that extend from the virus particle. Each particle has 12 homotrimeric fiber proteins, and thus, the receptor binding domain of the fiber (the knob) presents three separate binding sites.[14] Recently, the cellular receptor of Ad37 was found to be a glycoprotein carrying at least one terminal sialic acid moiety linked through an α(2−3) glycosidic bond to the neighboring saccharide chain. Thus, the ability of adenoviruses Ad8, Ad19, and Ad37 to cause EKC is strongly associated with their ability to bind to sialic acid on the cell surface.[15,16] An antiviral drug based on sialic acid might therefore have the potential to block viral attachment and therefore be used successfully to treat patients suffering from EKC. As discussed above, weak interactions between carbohydrates and proteins limit the use of carbohydrates as drugs. However, since EKC-

† Compound **17a**: PDB code 2WGT, structure factors r2wgtsf. Compound **17g**: PDB code 2WGU, structure factors r2wgusf.

* To whom correspondence should be addressed. Telephone: +46-786 9328. Fax: +46-90 786 7655. E-mail: mikael.elofsson@chem.umu.se.

‡ Department of Chemistry, Umeå University.

§ Department of Clinical Microbiology, Umeå University.

|| European Molecular Biology Laboratory.

[a] Abbreviations: Ad, adenovirus; EKC, epidemic keratoconjunctivitis; FITC, fluorescein isothiocyanate; FFU, fluorescent focus units; HATU, *O*-(7-azabenzotriazole-1-yl)-*N*,*N*,*N*′,*N*′-tetramethyluronium hexafluorophosphate; HCE cells, human corneal epithelial cells; HSA, human serum albumin; SA, sialic acid; SHEM, supplemented hormone epithelial medium.

10.1021/jm801609s CCC: $40.75
Published on Web 05/20/2009

Chart 1. HSA Conjugates of 3′-Sialyllactose and Sialic Acid

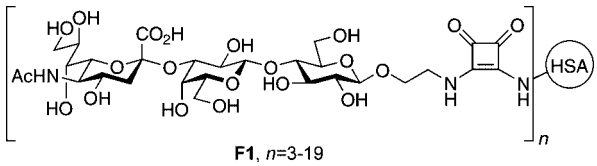

F1, *n*=3-19

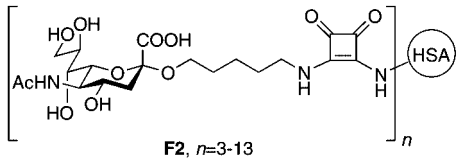

F2, *n*=3-13

causing adenoviruses attach to the host cells via multiple fiber proteins, it is possible that a drug could be prepared by using the multivalency approach, for example, using a glycoconjugate with several sialic acid derivatives linked to a protein carrier. The pharmacokinetic drawbacks of carbohydrate-based drugs are likely to be less severe in this case, since the potential drug would be administered directly to the eye, using a cream or eye drops. Naturally occurring, multivalent carbohydrates are often structurally complex and are generally only found in limited amounts in nature; they are therefore not preferred in drug development. By use of synthetic multivalent neoglycoconjugates instead, it is possible to control important structural properties such as the valency number, size, and flexibility of the conjugate.[17]

Recently, we reported two synthetic multivalent inhibitors (**F1**, **F2**, Chart 1) of the EKC-causing adenovirus Ad37.[18,19] The carbohydrate epitopes, coupled to an aminoalkyl spacer, were conjugated to human serum albumin (HSA) with varying degrees of valency by using squaric acid chemistry.[20−22] Biological evaluation of these compounds as inhibitors of Ad37 indicated an increased degree of inhibition with higher orders of multivalency and showed that multivalent conjugates effectively inhibit the binding of Ad37 to host cells and thereby prevent infection. The synthesis of the sialic acid-based inhibitor **F2** is more efficient than synthesis of the sialyllactose inhibitor **F1**. This is an important advantage in terms of time and cost of producing an antiviral drug. In addition, a smaller and less complex structure is generally easier to modify than a large structure.

In an attempt to optimize the inhibitory power of conjugate **F2**, we have now investigated the possibility of improving the binding affinity of sialic acid for the Ad37 fiber protein. On the basis of the crystal structure of the fiber knob protein of Ad37 in complex with sialyllactose,[23] we used structure-based design and docking to design a small library of 10 sialic acid derivatives in which the acetamide was replaced by different amides, urethanes, or ureas (Figure 1, structures **A**−**J**). We have developed a straightforward and efficient synthetic route to these compounds and their multivalent counterparts, i.e., corresponding HSA conjugates. The potency of these monovalent and multivalent structures as inhibitors of EKC-causing adenoviruses was evaluated in cell-binding assays, and the binding mode was studied by crystallization of sialic acid derivatives with the fiber knob protein of Ad37.

Results and Discussion

Structure-Based Design and Docking. Structure-based design was used to identify parts of sialic acid that can be varied

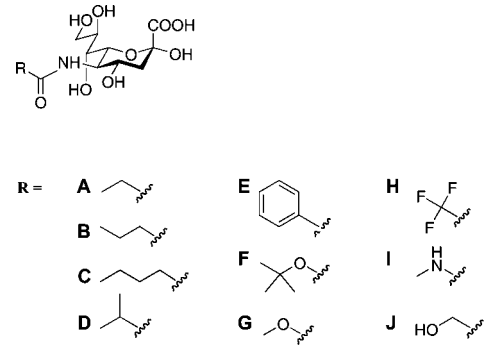

Figure 1. With the crystallographic structure of the sialic acid interacting knob domain of Ad37 in complex with 3′-sialyllactose, molecular modeling was used to design a library of 10 functionalized sialic acids (**A**−**J**).

in order to achieve a higher affinity of binding to the fiber knob of EKC-causing adenoviruses. From the crystallographic structure of the sialic acid-interacting knob domain of the Ad37 fiber protein in complex with sialyllactose, four main interactions between sialic acid and the protein were identified: one salt bridge, two hydrogen bond interactions, and one hydrophobic interaction (Figure 2). The axial carboxylic acid forms a salt bridge with the amino group of Lys345, the hydroxyl group in position 4 forms a hydrogen bond with the hydroxyl group of Tyr312, the amide group binds to the carbonyl group of Pro317 through a hydrogen bond, and the *N*-acetyl group of sialic acid is directed into a deep hydrophobic pocket formed by Tyr312, Tyr308 of another protein monomer, Pro317, and Val322.[23] We hypothesized that a bigger and more hydrophobic group, instead of the acetamide of sialic acid, would position itself in the hydrophobic cavity of the binding pocket and thereby improve the affinity because of increased hydrophobic interactions. Thus, we concentrated on optimizing this interaction between the hydrophobic pocket and the 5′-amide and keeping the rest of the sialic acid unchanged to ensure that the three important interactions mentioned above would be maintained. In order to obtain information about the limitations of the pocket in terms of size and shape, we docked a set of sialic acids where the acetamide was replaced with different amides, urethanes, or ureas (Figure 1, structures **A**−**E**) into the sialic acid binding site.[24] To validate the reliability of the dockings of the derivatives **A**−**E**, an initial docking of a new conformation of sialic acid into the binding site was performed. The calculated binding modes for sialic acid were compared with the experimental binding conformation of the sialic acid residue in sialyllactose. All docking poses were clustered within a 1.5 Å root-mean-square deviation (rmsd), indicating a strong consensus for a single binding mode similar to the experimental pose.[25] The results from the docking study of the functionalized sialic acids indicated that the deep hydrophobic cavity of the pocket was not as easy to enter as initially expected. A shelf at the mouth of the hydrophobic pocket forces derivatives with larger *N*-acyl substituents into major conformational changes, and the *N*-acyl substituents are not turned down into the large cavity as expected. The binding modes of these derivatives that are actually afforded are not likely to find the critical interactions discussed above. Except for sialic acid, the natural ligand, the best binding poses were observed for the propanamide derivative.

Figure 3A shows an overlay of the 10 best binding poses of the propanamide (displayed as line structures) with the sialic acid residue in the crystallographic structure of sialyllactose in complex with the Ad37 fiber protein (displayed as a capped stick structure). The majority of calculated poses were clustered

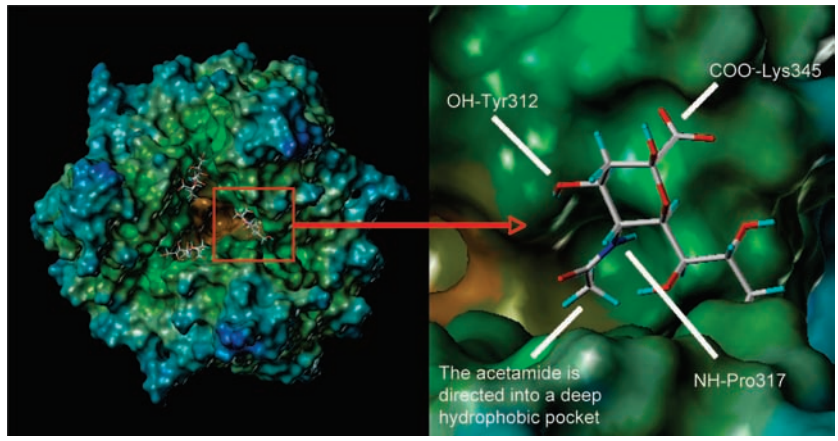

Figure 2. View of the sialic acid-interacting knob domain of the Ad37 fiber protein in complex with 3′-sialyllactose. The molecular surface of the fiber knob is colored blue for polar parts, brown for nonpolar parts, and green for intermediate polarity. Four main interactions between the sialic acid residue and the protein are highlighted:[23] one salt bridge (COO^-—Lys345), two hydrogen bonds (4-OH—Tyr312, 5-NH—Pro317), and one hydrophobic interaction between the *N*-acetyl group of sialic acid and the hydrophobic pocket formed by Tyr312, Tyr308 of another monomer, Pro317, and Val322.

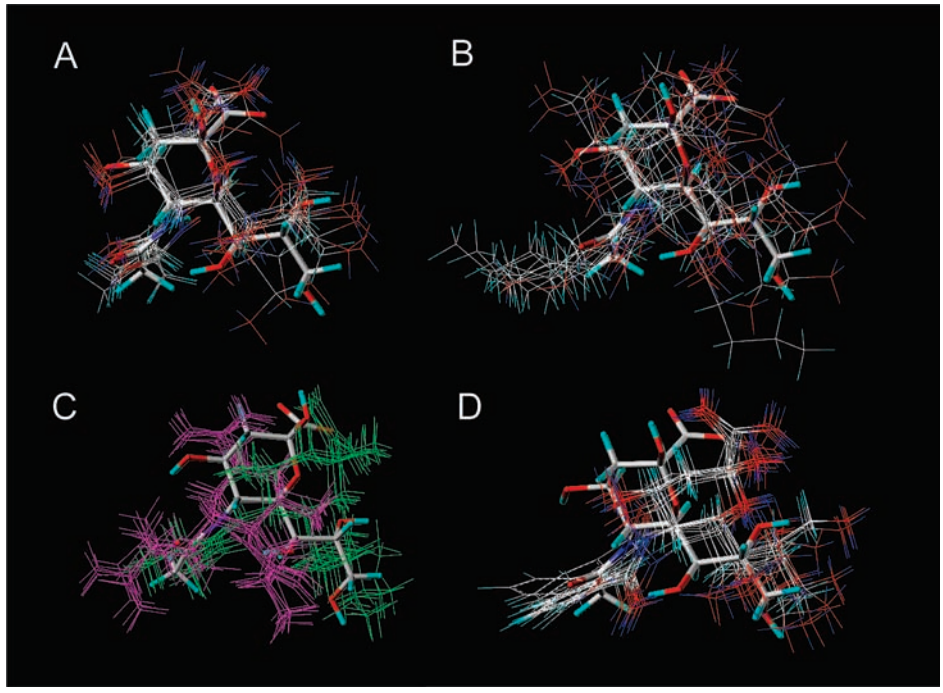

Figure 3. Overlays of the calculated binding poses for the functionalized sialic acids (displayed as lines) and the sialic acid residue of the experimental ligand (displayed as capped sticks). (A) The poses of the propanamide are clustered in a single binding mode close to the experimental ligand, indicating an affinity similar to that of sialic acid. (B) The poses of the pentanamide are spread out in the docked region of the binding site; thus, that derivative was predicted to be a poor binder. The poses of isobutanamide (C) and benzamide (D) are clustered in new binding modes with major differences compared to the experimental ligand, indicating other binding possibilities inside the binding site.

close to that of sialic acid and in a plausible conformation for finding the important hydrogen bond interactions discussed above. This strongly suggests that propanamide has a single binding mode, and this structure was therefore predicted to be a good binder with the ability to increase the binding affinity. With the extended derivatives, i.e., the butanamide and pentanamide, the docked poses were not clustered at all. They were found to be spread out in the entire docking region of the binding site, indicating that these structures have no specific binding mode. In addition, by overlaying of the docked positions on the experimental sialic acid residue, it could be seen clearly that these compounds would hardly find the important hydrogen bonding interactions. Thus, these compounds could be predicted to be poor binders. In Figure 3B, 10 representative docking poses of the pentanamide (lines) have been overlaid on the experimental structure (capped sticks). The poses of the benzamide and the isobutanamide differ from those of the other derivatives. According to the results with butanamide and pentanamide, we had expected that a larger substituent on the amide would cause a poor fit to the binding site, resulting in an extensive spread of the docking poses of the isobutanamide and the benzamide. Indeed, these amide substituents would be too big to enter the hydrophobic cavity and they are also positioned without any chance of finding the three important hydrogen bonds found for sialic acid, but interestingly, they are closely clustered—in one single binding pose for the benzamide and two binding poses for the isobutanamide (Figure 3C and Figure 3D). This might indicate a second possibility of binding inside the binding site.

Chart 2. Primary Synthetic Targets

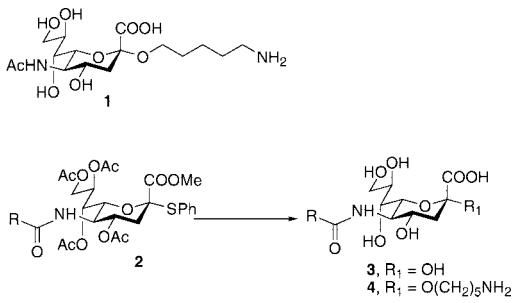

Although the propanamide was the only derivative predicted to have the ability to increase the affinity for the fiber protein of Ad37, we did not discount the possibility that any of the other derivatives might be active in a natural biological system. The predictions above are based on computer-simulated protein−ligand interactions, and the protein structure is a static model of a dynamic structure. As with most docking approaches, the docking algorithm used in this study only allows the ligand and the hydrogens of the protein to be flexible and considers the protein to be rigid. Thus, features such as induced fit or other conformational changes that could occur upon binding are not taken into account and structures other than the propanamide could actually fit inside the binding site.[26] In order to get as much information as possible about the effect when the acetamide is replaced, we decided to synthesize a set of sialic acid derivatives that were predicted to range from poor to good binders compared to sialic acid. The set contains all the hydrophobic amides from the docking study and also small and hydrophilic functionalities that were not docked (Figure 1).

Synthesis. In our previous work with the synthetic multivalent inhibitor **F2** (Chart 1), we used sialic acid derivative **1** (Chart 2) that was conjugated to a protein carrier by the aminopentyl spacer.[19] In the present study we intended to use the same synthetic strategy to afford multivalent conjugates of selected parts of the library, and therefore, the sialic acid derivative **2** (Chart 2) was chosen as a target structure. From **2**, we planned to synthesize both functionalized sialic acids **3** (Chart 2) and also the aminopentyl derivative **4** (Chart 2) that can be conjugated to HSA.

Synthesis of *N*-Acyl Functionalized Sialic Acids. Commercial sialic acid was used as starting material, and synthesis of the sialic acid thiophenyl derivative **5** (Scheme 1) was performed according to published procedures.[27,28] In order to functionalize **5**, the amine was first Boc-protected and then deacetylated; this was followed by O-reacetylation to get **6**.[29] Transformation to the amides **2a**−**h** was then performed by removal of the Boc group with TFA in CH_2Cl_2, directly followed by acylation of the amine. For the derivatives **2a**−**e**, we used the corresponding anhydride in the presence of a base, and to get derivatives **2f**, **2g**, and **2h**, we used benzoic acid, methyl chloroformate, and methylisocyanate, respectively. The coupling reactions were followed by LCMS. The larger anhydrides required longer coupling times, and they also resulted in lower yields due to *O*- to *N*-acetyl migration. In order to minimize the amount of side products, the reaction was stopped when the formation of the main product ceased, despite there being some remaining starting material in the mixture. The crude products were purified by column chromatography and also preparative HPLC when necessary. The target derivatives **2a**−**h** were obtained in yields ranging from 52% to 89%, calculated from **6**.

The deprotection of **2a**−**h** to their corresponding sialic acids was planned to go through three steps: hydrolysis of the SPh group by NIS, H_2O, and MeCN, deacetylation of the *O*-acetates with methanolic sodium methoxide, and finally hydrolysis of the methyl ester by LiOH. This strategy was initially tried out for the derivatives **2a** and **2b**. The first step was quite straightforward, and **7a** and **7b** were obtained in 60% and 84% yields, respectively. After deacetylation and hydrolysis of **7a** and **7b** with LiOH, however, the sialic acids expected (**3a** and **3b)** could not be isolated. Instead, a product with a completely different ^{1}H NMR spectrum was observed. By careful investigation of LCMS chromatograms and ^{1}H NMR spectra of the products obtained and by extensive search of the literature, we found a feasible explanation. According to published investigations of the thermal and physical stability of sodium *N*-acetylneuraminate,[30] degradation of sialic acid can occur under thermal alkaline conditions whereby the sialic acid ring structure is degraded. Although the hydrolysis was performed at room temperature, all the chromatographic and spectroscopic data indicate that deprotection of **7a** and **7b** resulted in an inseparable mixture of the target sialic acids **3a** and **3b** and the degraded derivatives **9a** and **9b**. Despite several attempts to avoid this transformation, it was not possible to synthesize fully deprotected *N*-acyl modified sialic acids. However, for future purposes the deprotected thiophenyl derivatives **10a**−**i** have been synthesized in 44−94% yield from **2a**−**h** and **6** by convenient deacetylation and hydrolysis.

In order to find a new strategy for the synthesis, it was decided to base the library on the methyl glycoside of sialic acid **11** (Scheme 2) that was synthesized from sialic acid by published procedures.[31] From the crystallographic structure of the sialic acid-interacting domain of Ad37 in complex with sialyllactose, we have already shown that the lactose residue of 3′-sialyllactose is directed out of the binding site toward the environment.[23] Thus, we hypothesized that an α-methyl glycoside instead of an α-hydroxyl group in the anomeric position would not change the binding properties of the derivatives. To verify this hypothesis before we started the synthesis of this second library, we ran a cell-binding assay to compare the methyl glycoside of sialic acid with sialic acid regarding their potential to inhibit adenoviral adhesion to HCE cells. As expected, the results showed no significant difference in inhibitory power (data not shown).

Functionalization of the methyl glycoside **11** was performed in four steps. The amine **15** was obtained by a procedure similar to that discussed for the thiophenyl derivatives above. A *t*-butoxycarbonyl group (Boc) was added to the acetamide, and deacetylation of **12** was performed with methanolic sodium methoxide. Column chromatography of the crude residue gave the pure α isomer **13** in 65% yield from **11**. The α-anomeric configuration was established by determination of the coupling constant between C1 and $H3_{ax}$ ($J = 6.63$ Hz).[32] Compound **14** was obtained in 92% yield after reacetylation of the hydroxyl groups by Ac_2O in pyridine.

Prior to the amide-functionalizing step, the Boc group was removed with TFA in CH_2Cl_2, resulting in the free amine as TFA salt (**15**), which was used immediately without any purification. The synthesis of **16a**−**h** was generally performed using traditional amide coupling synthesis with activated carboxylic acids. The carboxylic acid, HATU, and DIPEA were added to the amine **15** in CH_2Cl_2 and stirred at room temperature until no further reaction was observed with LCMS. The use of activated carboxylic acids instead of anhydrides (Scheme 1) shortened the coupling reaction time and minimized acetyl

Scheme 1. Synthesis of Amide-Functionalized Sialic Acids[a]

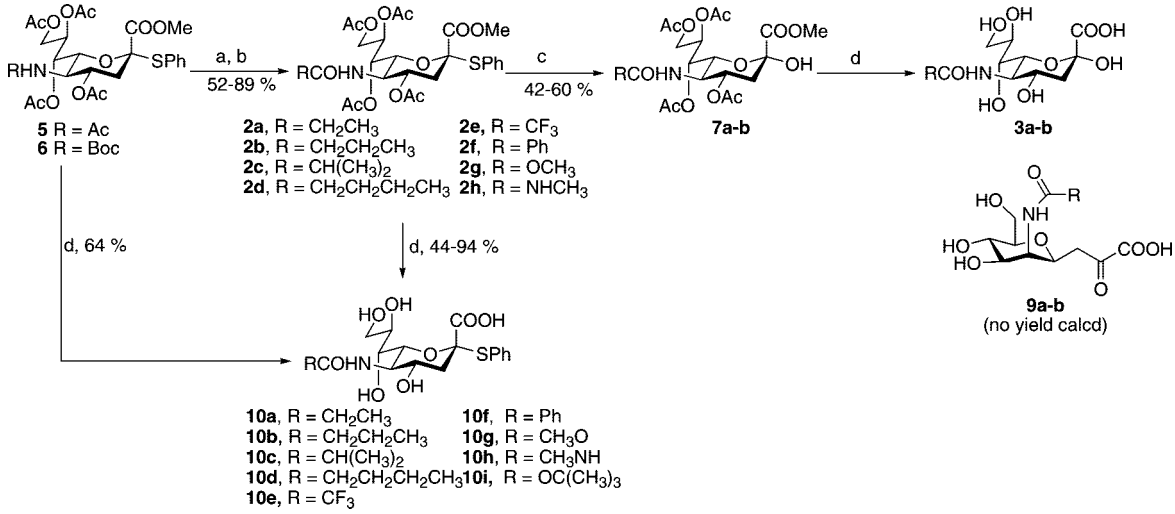

[a] Reagents and conditions: (a) 90% TFA (aq), CH_2Cl_2, room temperature, 1−2 h. (b) **2a**−**e**: $(RCO)_2O$, DMAP, CH_2Cl_2, room temperature, 5−11 h. **2f**: PhCOOH, HATU, DIPEA, CH_2Cl_2, room temperature, 3 h. **2g**: CH_3OCOCl, DIPEA, CH_2Cl_2, room temperature, 1 h. **2h**: CH_3NCO, DIPEA, CH_2Cl_2, room temperature, 4 h. (c) NIS, MeCN/H_2O 10:1, room temperature, 3 h; (d) (1) NaOMe, MeOH, room temperature, (2) LiOH (aq) MeOH, room temperature.

Scheme 2. Synthesis of Amide-Functionalized Sialic Acid Methyl Glycosides[a]

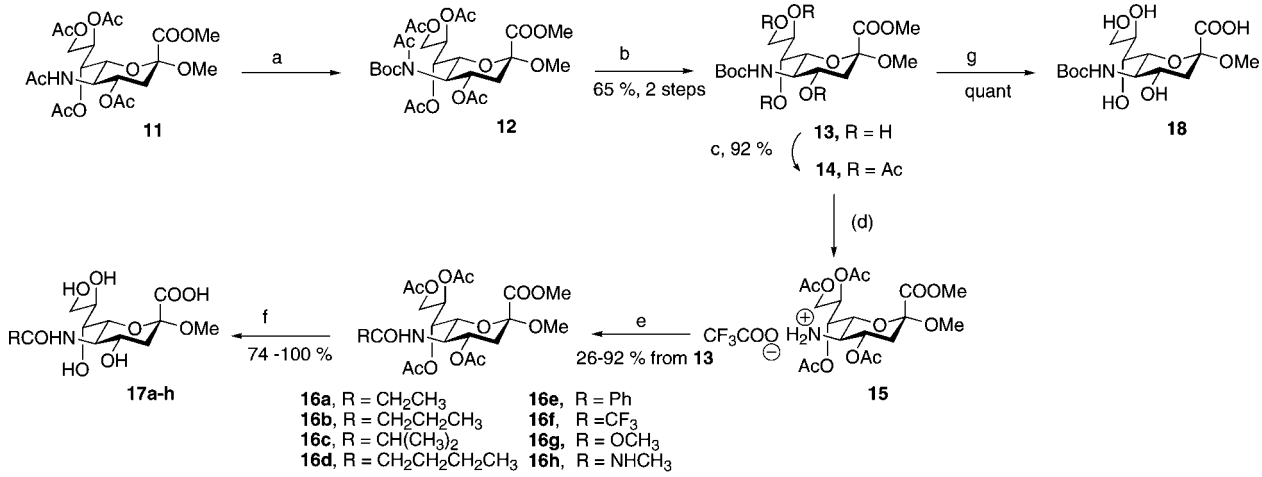

[a] Reagents and conditions: (a) Boc_2O, DMAP, THF, reflux, 2 h; (b) NaOMe, MeOH, room temperature, 3 h; (c) Ac_2O, Py, room temperature, overnight; (d) 90% TFA (aq), CH_2Cl_2, room temperature, 1−2 h. (e) **16a**-**e**: RCOOH, HATU, DMAP, CH_2Cl_2, room temperature, 3−5 h. **16f**: $(CF_3CO)_2O$, DMAP, CH_2Cl_2, room temperature, 0.5 h. **16g**: CH_3OCOCl, DIPEA, CH_2Cl_2, room temperature, 1.5 h. **16h**: CH_3NCO, DIPEA, CH_2Cl_2, room temperature, 4 h. (f) (1) NaOMe, MeOH, room temperature, 2 h, (2) 2 M LiOH (aq), MeOH, room temperature, overnight; (g) 2 M LiOH (aq), MeOH, room temperature, overnight.

migration. We nevertheless obtained low yields and acetate migration for the most hydrophobic amides **16c** and **16d**. To get **16f**, **16g**, and **16h**, we used methyl chloroformate, methyl isocyanate, and trifluoroacetanhydride, respectively. In order to obtain pure products, extensive purification by repeated column chromatography was necessary. All derivatives were obtained with reasonable yields (26−92%). With the methyl glycoside instead of the free hydroxyl group at the anomeric position, there were no difficulties with the deprotection. The fully deprotected compounds **17a**−**h** were obtained in 74−100% yield after O-deacetylation with methanolic sodium methoxide and methyl ester hydrolysis with LiOH. Unfortunately, **17f** was obtained as an inseparable mixture with the corresponding free amine and was therefore excluded from the library. The unprotected Boc derivative **18** was easily obtained by hydrolysis of **13** in quantitative yield.

Synthesis of Multivalent *N*-Acyl Functionalized Sialic Acids. In order to investigate the differences in inhibitory power of *N*-acyl modified sialic acids further, the multivalent counterparts of **17a**−**c** were synthesized and evaluated. It was assumed that the sialic acid derivatives would display differences in affinity for the fiber knob protein and that the differences would be enhanced by multivalency. The multivalent compounds **22a**−**c** were synthesized from sialic acid derivative **6**[19] (Scheme 3). In order to minimize the amount of synthetic work, we decided to elongate **6** with the aminopentyl spacer needed for further conjugation to HSA, before diversifying the sialic acid amide. Commercially available Fmoc-aminopentanol was glycosylated with compound **6**[19] to give the pure α-isomer **19** in 68% yield after extensive purification. The α-anomeric configuration of **19** was established by determination of the coupling constant between C1 and $H3_{ax}$ ($J = 5.9$ Hz). The amide functionalizing step to **20a**−**c** followed the carboxylic acid/HATU procedure described above, and the amides were obtained in 18−64% yield. In addition, it was found that methyl ester hydrolysis and partial deacetylation occurred during Boc removal according to LCMS analysis. This in part explains the modest yield of the amide couplings, both in this case and for

Scheme 3[a]

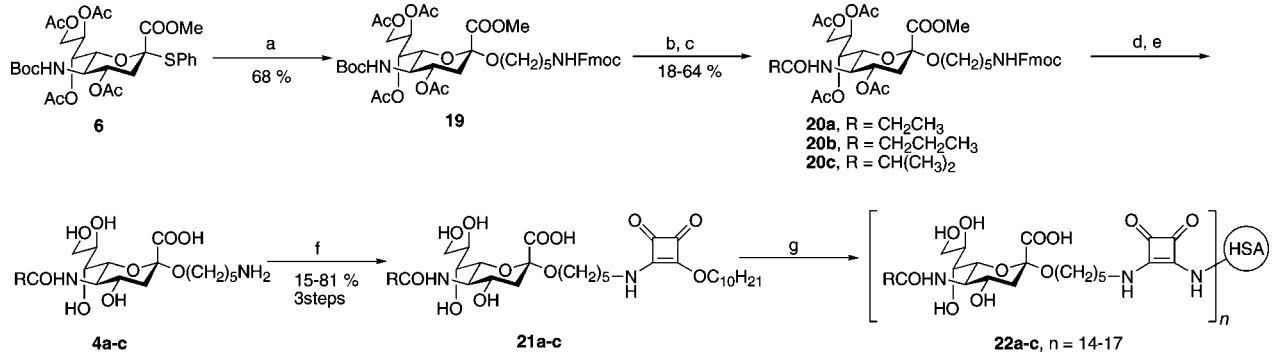

[a] Reagents and conditions: (a) Fmoc-aminopentanol, molecular sieves (3 Å), AgOTf, 1 M IBr in CH_2Cl_2, CH_3CN/CH_2Cl_2 (3:2), −72 °C, 4 h; (b) 90% TFA (aq), CH_2Cl_2, room temperature, 1 h; (c) RCOOH, HATU, DIPEA, CH_2Cl_2, room temperature, 9−24 h; (d) NaOMe, MeOH, room temperature, 1 h; (e) LiOH (aq), MeOH, room temperature overnight.; (f) didecyl squarate, DMF, Et_3N, room temperature, 11 h; (g) $NaHCO_3$, HSA (human serum albumin), room temperature, 27 h.

Table 1. Evaluation of *N*-Acyl Modified Sialic Acids **17a**−**h** (**17f** Excluded), **18**, and Commercial NeuGc as Inhibitors of Ad37 Attachment to HCE Cells[a]

compd	run 1	run 2	run 3
SA	+ +	+ +	+ +
17a	+ +	no data	+ +
17b	−	+	−
17c	−	−	no data
17d	−	+	−
17e	+	+ +	+
17g	+ +	+	−
17h	+	−	+
18	−	−	−
NeuGc	−	−	−

[a] Compounds are denoted + + if they were effective as inhibitors to the same extent as sialic acid or more, + if they were less potent than sialic acid, and − if they had no effect at all. Each experimental run consisted of a duplicate dilution series of each compound (2, 4, 8, and 16 mM), and the data represent the average of duplicate determinations (for experimental details, see Supporting Information).

the monovalent library described above. The amides **20a**−**c** were fully deprotected under standard conditions, and the crude products **4a**−**c** were used in the following conjugation step without further purification. Conjugation of **4a**−**c** to HSA was performed by the squaric acid strategy,[20−22] and the intermediate squaric decyl ester sialosides **21a**−**c** were obtained in 15−81% yield. The three neoglycoproteins **22a**−**c** were subsequently obtained with 14, 16, and 17 saccharides incorporated per HSA, respectively. The average degree of incorporation was determined by MALDI-TOF MS using the center of the single-charged neoglycoprotein peak. This was confirmed with gel electrophoresis.

Biological Evaluation. In order to investigate whether the modified sialic acids synthesized above could prevent attachment of Ad37 virions to HCE cells, a cell-binding assay based on ^{35}S-labeled virions was used (Table 1).[33−35] S-Labeled virions were preincubated with commercial sialic acid or the synthesized *N*-acyl modified α-methylsialosides **17a**−**h** (**17f** excluded), **18**, or NeuGc (*N*-glycolylneuraminic acid) before adding the virions to HCE cells. After incubation, unbound virions were washed away and cell-associated radioactivity was measured. The experiment was repeated three times. Because of large standard deviations and variation in results, it was only possible to make a rough estimate of the activity of the compounds. The results are presented in Table 1 and show that the propanamide **17a**, which was predicted to be a good inhibitor according to the docking study, was as efficient as sialic acid in preventing attachment of Ad37 to cells. In addition, the methylcarbamate **17g** and the benzamide **17e** were slightly efficient as inhibitors, whereas all of the other sialic acids with large *N*-acyl substituents had no effect at all. An assay that shows Ad37 infected cells as fluorescent focus units (FFU) was used to investigate whether the compound could prevent infection (Figure 4).[15,35] Unlabeled Ad37 virons were preincubated with a dilution series of sialic acid or the *N*-acyl modified sialic acids **17a**,**b**,**c**,**e**,**g** before being incubated with HCE cells. Unbound virions were washed away, and cell-associated virions were allowed to infect the cells. Thereafter, the cells were incubated with rabbit polyclonal anti-Ad37 serum followed by FITC (fluorescein isothiocyanate) conjugated swine antirabbit IgG antibodies and examined with an immunofluorescence microscope. The results confirmed the activity of the propanamide **17a** and the methyl carbamate **17g**. Both prevented Ad37 from infecting the cells to the same extent as sialic acid, or more. The benzamide **17e**, on the other hand, had no effect in this assay. The *N*-acyl modified sialic acids **17b** and **17c** had no effect in the cell-binding assay, and as expected, they were inactive in the infection assay. For several of the compounds, most notably **17b**, **17c**, and **17e**, infection was enhanced when the concentration of compound was increased from 1 to 2 mM. The underlying reason for this is, however, unknown. The multivalent HSA conjugates **22a**−**c** were also evaluated in the cell infectivity assay (Figure 5). As expected, the multivalent *N*-acyl modified sialic acids followed the behavior of their monovalent counterparts. The conjugates with large *N*-acyl substituents, **22b** and **22c**, did not prevent Ad37 from infecting HCE cells. The multivalent propanamide **22a** was active as an inhibitor, with a clear multivalency effect. However, **22a** was much less efficient than multivalent sialic acid (17-valent), and thus, sialic acid remains the most efficient inhibitor of EKC-causing adenoviruses.

Crystallography. X-ray crystallography was used to investigate the exact binding of **17a**, **17e**, and **17g** to the fiber protein of Ad37 at the molecular level. From the results of the docking study and the biological evaluation of these compounds, **17a** and **17g** bind to the Ad37 fiber knob in a fashion similar to that of sialic acid, whereas the benzamide **17e** may interact with the fiber knob in a different way.

Cocrystals of the Ad37 fiber knob in complex with each ligand were grown by the hanging drop method.[23,45] Data were collected using synchrotron radiation and the crystals diffracted to 1.8 Å resolution. The structures were solved by molecular replacement using the previous structure of the complex of Ad37−sialyllactose[45] (Table 2). As control, crystals with sialyllactose were reproduced. The ligand **17e** was not visible

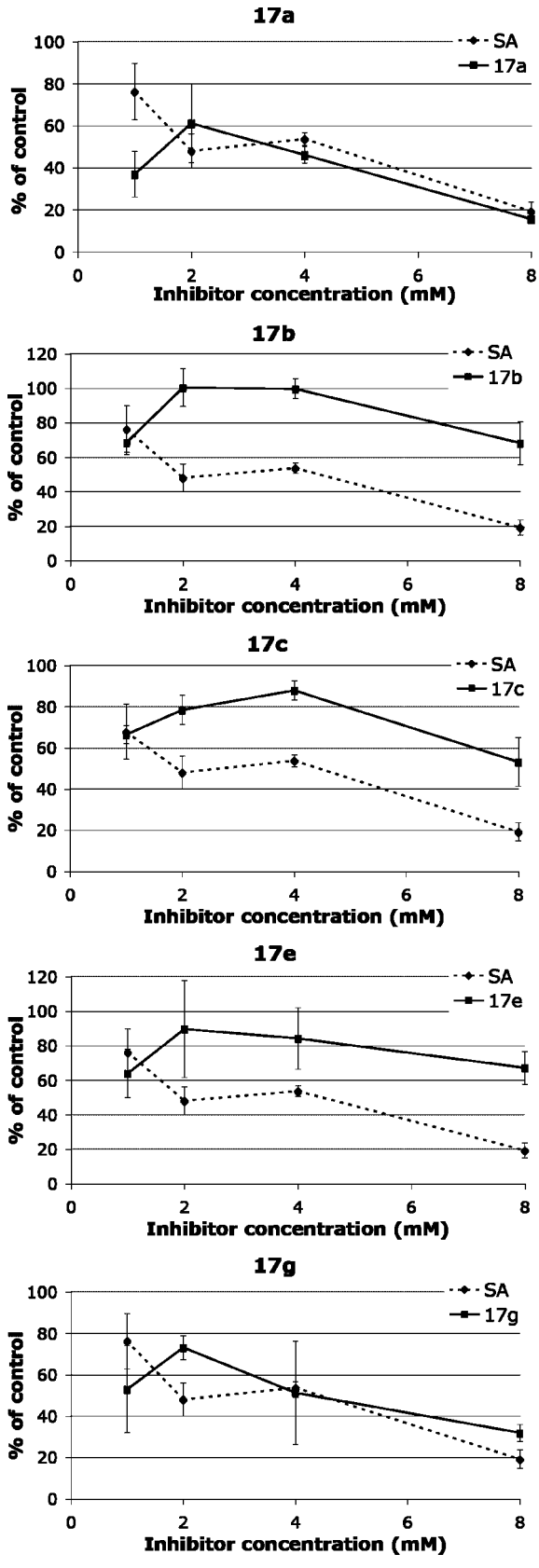

Figure 4. Dose-dependent inhibition of Ad37 infection of HCE cells by *N*-acyl modified sialic acids **17a**, **17b**, **17c**, **17e**, and **17g** (black lines), compared to sialic acid (SA, dashed lines). The derivatives **17a** and **17g** were as effective at inhibition as sialic acid, while **17b**, **17c**, and **17e** were inactive. The data represent the average of duplicates within one experiment, and the experiment was repeated twice with reproducible results (for experimental details, see Materials and Methods).

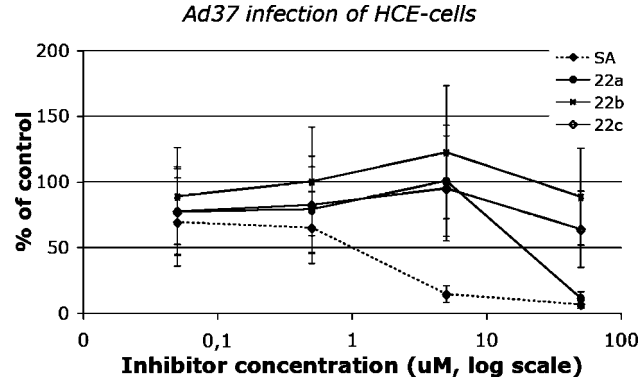

Figure 5. Dose-dependent inhibition of EKC-causing adenoviruses by 17-valent sialic acid and the multivalent *N*-acyl modified sialic acids **22a**−**c** (14- to 17-valent). The experiment was repeated three times with reproducible results. The data represent the average of duplicates for each dilution series (for experimental details, see Materials and Methods).

Table 2. Data Collection and Refinement Statistics for Structures of Ad37 Fiber Protein in Complex with the Modified Sialic Acids **17a** and **17g**

	17a	**17g**
space group	$P2_1$	$P2_1$
unit-cell dimensions		
a (Å)	61.27	61.14
b (Å)	69.99	69.93
c (Å)	75.00	74.45
β (deg)	94.42	94.35
resolution range[a] (Å)	30−1.8 (1.80−1.90)	30−1.80 (1.80−1.86)
R_{merge}[a]	4.5 (46.7)	5.3 (60.8)
$I/\sigma(I)$[a]	18.39 (2.88)	13.85 (1.84)
completeness (%)[a]	99.8 (99.8)	99.3 (98.2)
no. of unique reflections	58545	57656
Refinement		
resolution range[a] (Å)	30−1.80 (1.80−1.85)	30−1.80 (1.80−1.85)
total no. reflections/free	55584/2953	54725/2931
R_{work}[a]	0.183 (0.261)	0.183 (0.304)
R_{free}[a]	0.226 (0.284)	0.223 (0.387)
average *B*-factor (Å^2)	19.4	19.2
no. water molecules	721	674
Root-Mean-Squared Deviation		
bond lengths (Å)	0.010	0.012
bond angles (deg)	1.225	1.339
Ramachandran Plot[b]		
favored (%)	96.5	96.5
allowed (%)	99.3	99.3

[a] Values in parentheses are for highest-resolution shell. [b] Molprobity http://molprobity.biochem.duke.edu/.

in the structure of the known binding site of sialic acid or anywhere else in the fiber protein, indicating no binding. The potential of **17e** as an inhibitor of Ad37 attachment (Table 1) most likely results from unspecific binding to the fiber protein. In contrast, **17a** and **17g** were both clearly observed within the sialic acid binding site and with well-defined electron density (Figure 6). Overlays with the Ad37−sialyllactose complex showed that both **17a** and **17g** were positioned in the same orientation as sialic acid. All of the important interactions were fulfilled, and as predicted, the propanoyl and methoxycarbonyl groups were directed into the hydrophobic part of the binding site. From the crystallographic structures, it was also evident that **17a** and **17g** were slightly shifted in comparison to sialic acid while the amino acid residues in the binding pocket were unaffected by the variation in structure between the different ligands. In addition, the crystallographic structures suggest that

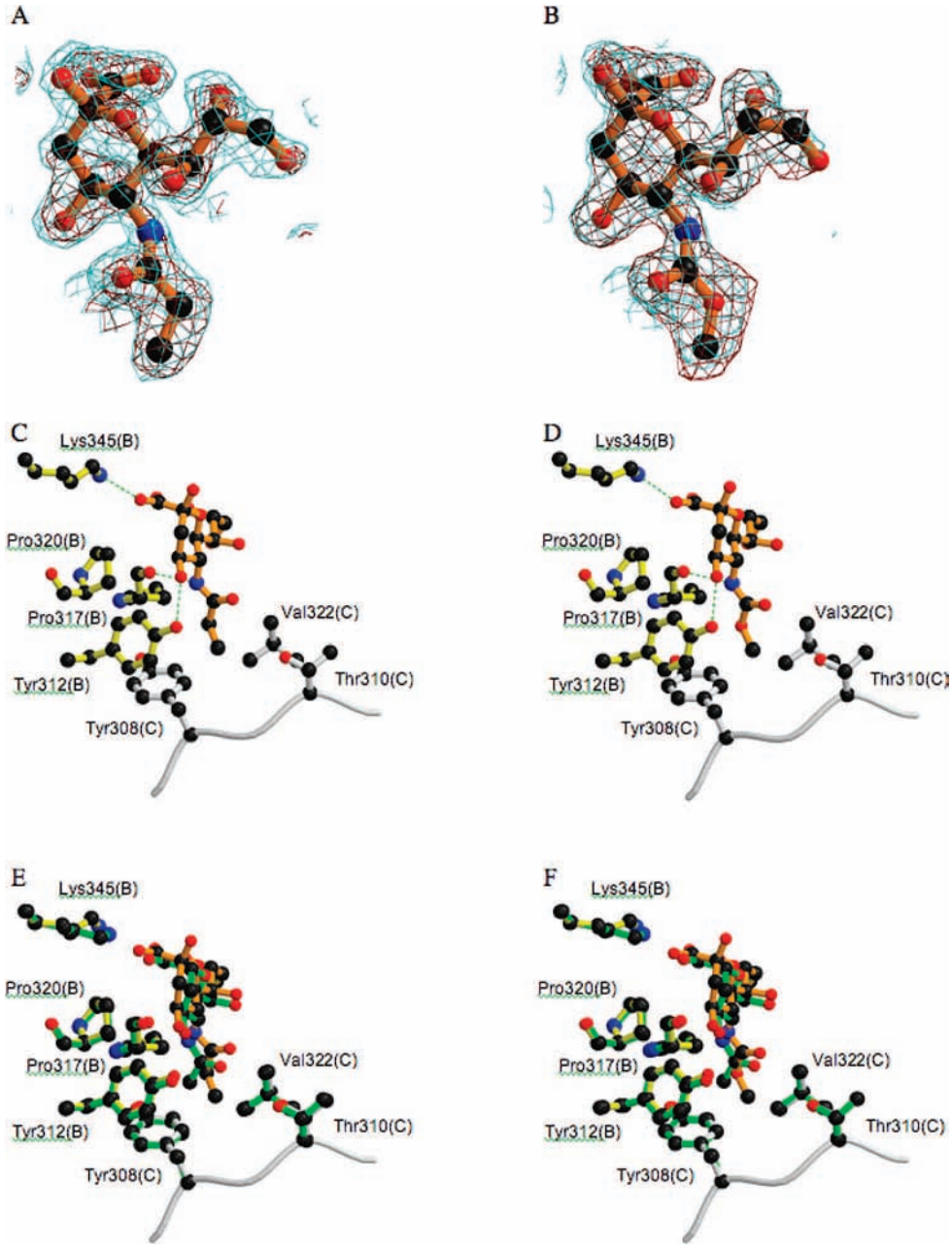

Figure 6. Crystallographic structures of the *N*-acyl modified sialic acids **17a** (A, C, E) and **17g** (B, D, F), in complex with the Ad37 fiber knob protein were solved to 1.8 Å resolution by molecular replacement. Both ligands were seen with well-defined electron density (A, B) within the binding site of sialic acid (C, D). Superposition with the sialyllactose−Ad37 structure (E, F) shows that the *N*-acyl modified sialic acids bind to the binding site in a similar manner as sialic acid, with the extra atoms on the *N*-acyl group directed down to the hydrophobic part of the binding site: (A, B) black electron density map, unbiased difference density (2.50σ); blue, final refined map (0.95σ); (C−F) white and yellow residues, chain C and chain B, respectively, of the homotrimer of the Ad37 fiber protein in presence of the *N*-acyl modified sialic acids; orange sticks, *N*-acyl modified sialic acids; (E, F) green, sialic acid and surrounding residues from the sialyllactose−Ad37 structure.

larger groups such as a butanoyl moiety could readily be accommodated in the hydrophobic pocket. The experimental data on virus attachment and infection for the butanoyl derivative **17b** do, however, indicate that this pocket is not fully accessible.

Conclusions

In previous studies, we have shown that multivalent sialic acid conjugates are effective inhibitors of EKC-causing adenoviruses.[18,19] In this study, structure-based design was used to increase our understanding of the sialic acid−Ad37 interaction. Using the crystallographic structure of sialyllactose in complex with the fiber knob protein of Ad37, we found that the acetamide of sialic acid is directed into a deep hydrophobic pocket. A set of 10 *N*-acyl modified sialic acids was designed, synthesized, biologically evaluated, and compared to sialic acid. The *N*-acyl modified sialic acids were synthesized as their α-*O*-methyl glycosides (**17a**−**h** and **18**). They were synthesized in seven steps from the methyl glycoside of sialic acid in 12−65% total yield. Biological evaluation of these compounds in a cell binding assay and a cell infection assay revealed that only sialic acids with small *N*-acyl groups were effective as inhibitors of attachment of Ad37 to and infection of HCE cells. The propanamide **17a** and the methyl carbamate **17g** were almost as efficient as sialic acid in this respect. In order to investigate the capabilities of *N*-acyl substituted sialic acids further, the multivalent HSA conjugates **22a**−**c** were synthesized and

evaluated. An efficient synthetic strategy to obtain the multivalent HSA conjugates was developed, and they were obtained in seven steps from the 2-thiophenyl donor of sialic acid in 10−32% yield. The degree of multivalency was determined to be 14−17 saccharides incorporated per HSA. The multivalent butanamide **22b** and the isobutanamide **22c** showed no activity. The multivalent propanamide **22a**, which was as potent as sialic acid in the monovalent case (**17a**), was much less effective than multivalent (17-valent) sialic acid. From these results, it is obvious that the hydrophobic cavity of the binding site is not as easy to occupy as initially expected. Crystallography confirmed that **17a** and **17g** bind in the same orientation as sialic acid. It seems likely that the sialic acid interacting site of Ad37 is very rigid and not prone to any conformational changes to fit the larger substituents.

Future efforts to obtain a high-affinity structure as an inhibitor of EKC-causing adenoviruses will require more extensive structure−activity investigations. Because of the complicated synthesis of functionalizing sialic acid, an alternative strategy for development of successful inhibitors might be replacement of the entire sialic acid core with a non-carbohydrate sialyl mimetic presenting the critical attributes for viral recognition. A non-carbohydrate sialyl mimetic would be more advantageous than functionalized sialic acids in terms of less complicated synthesis and a greater possibility of varying the functional groups. The results presented here would be valuable for future efforts to develop an antiviral drug for treatment of EKC, regardless of whether it is via the sialic acid strategy or by using sialyl mimetics.

Materials and Methods

Computational Methodology. Pretreatment of Protein. The three-dimensional coordinates of the fiber knob protein of Ad37 were obtained from the Protein Data Bank (code 1UXA). All hydrogens were first removed from the PDB file and then added again using the software Reduce,[36] after which the orientations of the side chains of ASN, GLN, and HIS were optimized. Protonation states were set according to the program, based on the likelihood that the residues would be charged at physiological pH, together with their opportunities to form hydrogen bonds with the surrounding environment. All water coordinates and metal complexes were removed from the protein file. Important residues, especially in the binding site, were visually inspected and corrected according to charge and according to atom and bond type.

Pretreatment of Ligand. The ligands that were selected for the docking studies were drawn using CS Chemdraw Ultra[37] software and represented as SMILES.[38] Their 3D structures were generated with CORINA.[39] All ligands were inspected and refined to correct stereochemistry and atom and bond type according to GOLD (genetic optimization for ligand docking)[40] specifications using MOE (Molecular Operating Environment)[41] and SYBYL[42] software. In order to obtain low-energy conformations for all ligands, they were energy-minimized using the MMFF94 force field implemented in MOE.

Energy Minimization of the Binding Site. The protein−ligand complex of one of the three binding sites presented by the Ad37 fiber protein was energy-minimized using the Amber94 force field on the 3′-sialyllactose ligand and its surroundings within a distance of 3 × 4.5 Å (corresponding residues were also included). The binding site and the ligand were then visually examined to confirm that the conformations were plausible. Before docking, the ligand was removed from the binding site.

Docking in GOLD. In GOLD, the ligands are placed in the protein binding site by a mechanism based on fitting points. A genetic algorithm (GA) is used to explore possible binding modes, and a scoring function is used to rank the calculated binding modes.[25,43,44] In this study, the default settings of the GA parameters were used with the Goldscore scoring function. The docking region was enclosed by a sphere of 10 Å centered on the center of gravity of the sialic acid residue of the experimental ligand. Each ligand was docked into the binding site in 20 GA runs, resulting in 20 binding poses per ligand. To test the reliability of the poses generated by GOLD, the ability to reproduce the experimental binding mode of the sialic acid residue of the experimental ligand was tested. The experimental ligand was taken out of the X-ray structure, and a new conformation of sialic acid was docked back into the binding site using the settings above. An average rmsd value of 1.5 Å between the 20 calculated poses and the experimental pose indicates a reliable prediction of the binding mode.[25]

Evaluation of the Docking. All docking poses for all ligands were evaluated visually. The docked poses were overlaid on the experimental ligand in the binding site using the software SYBYL.[42] Compounds with a majority of the calculated poses were clustered close to the experimental binding mode of sialic acid and in a reliable conformation allowing the critical hydrogen bonds, and the salt bridge was defined as good binders with potential to increase the binding affinity. Compounds with the docked poses spread out in the binding site and not clustered at all were assumed to have unspecific binding modes and were predicted to be poor binders.

Biological Evaluation. The binding assay[33,34] and the infectivity assay[15,35] were carried out essentially according to the indicated literature procedures. See Supporting Information for details.

Protein Expression and Purification. Ad37 fiber knob DNA corresponding to residues 177−365 of the full-length fiber was cloned into the pPROEX HTb plasmid. The protein was expressed in the BL21 Star (DE3) bacterial strain in LB medium at 37 °C for 4 h after induction with 1 mM IPTG. The pellet was resuspended in buffer (150 mM NaCl, 30 mM Tris, pH 7.5) and incubated with lysozyme (1 mg/mL) on ice for 30 min and sonicated 12 times for 10 s each time. After centrifugation at 45000*g* for 30 min at 4 °C, the cleared lysate was loaded onto 10 mL of Ni Sepharose resin in a column in the presence of 10 mM imidazole, washed first with 50 mL of 150 mM NaCl, 30 mM Tris, pH 7.5, 10 mM imidazole and then with 40 mL of 150 mM NaCl, 30 mM Tris, pH 7.5, 20 mM imidazole and then eluted in several 5 mL fractions with buffer (150 mM NaCl, 30 mM Tris, pH 7.5, 0.5 M imidazole). The His tag was cleaved off by an overnight incubation with a $^{1}/_{100}$ dilution of His-tagged TEV protease at 10 °C. Imidazole was eliminated by dialysis against the buffer 150 mM NaCl, 30 mM Tris, pH 7.5, 20 mM imidazole. Cleaved protein was then incubated with 5 mL of Ni Sepharose for 1 h at 4 °C and recovered in the flow-through and washing fractions ((5−6) × 5 mL). These fractions were pooled, concentrated to 7−8 mg/mL, and purified over a Superdex 200 column, and the peak collected was concentrated to 15 mg/mL for crystallization.

Crystallization and Structure Determination. Cocrystals of Ad37 fiber knobs (at 13 mg/mL) with each ligand were grown by the hanging drop method[23,45] using a reservoir solution of 25−27% polyethylene glycol 8000, 50 mM zinc acetate, and 100 mM HEPES (pH 7.15, 7.3, or 7.5). Crystals were fast-frozen in nitrogen prior to data collection without cryoprotection. Data were collected on beamline ID14-2 and ID14-4 at the European Synchroton Radiation Facility (Grenoble, France). As a control, crystals with 20 mM sialyllactose were reproduced.[23] The best diffraction was obtained with crystals grown under conditions of 25% PEG 8000, 50 mM zinc acetate, and 100 mM HEPES, pH 7.5. Data were collected on ID14.4 beamline at 1.8 Å resolution. For **17a**, **17e**, and **17g** the best diffracting crystals were grown in the presence of 20 mM ligand in the same crystallization condition as for sialyllactose. Data were collected on ID14-eh2 beamline at 1.8 Å resolution. The structure was solved by molecular replacement using the Ad37−sialic acid structure. Data collection for **17e** at 1.8 Å resolution and structure resolution were performed in the same way, but the ligand was not visible in the structure at the known site for sialic acid. The best diffracting crystals were grown in the presence of 10 mM ligand in crystallization solution 27% PEG 8000, 50 mM zinc acetate, and 100 mM HEPES, pH 7.5. Data collection at 1.8 Å resolution and structure resolution were performed in the same way

as before, but the ligand was not visible in the structure at the known site for sialic acid.

Chemical Synthesis. Methyl (*O*-Methyl-5-(*N*-*tert*-butoxycarbonylacetamido)-4,7,8,9-tetra-*O*-acetyl-3,5-dideoxy-D-glycero-α-D-galacto-2-nonulopyranosyl)onate (12). A solution of **11**[31] (1.81 g, 3.6 mmol, 4:1 α/β), Boc_2O (1.8 mg, 8.2 mmol), and 4-dimethylaminopyridine (DMAP) (267 mg, 2.2 mmol) in dry THF (60 mL) was refluxed for 2 h under nitrogen. The reaction was followed by TLC (toluene/ethanol 10:1). The reaction mixture was cooled to room temperature, diluted with CH_2Cl_2, washed with 0.5 M aqueous HCl, water, saturated $NaHCO_3$ (aq), and water, dried, and concentrated. Column chromatography (toluene/ethanol 10:1) gave 2.1 g of product **12** as a yellow oil, still as a 4:1 α/β mixture and with additional 10% of impurities. Since the impurities as well as the β isomer were removed in later steps, this product was used despite having impurities. Thus, no yield and no NMR data are presented.

Methyl (*O*-Methyl-5-(*N*-*tert*-butoxycarbonyl)-3,5-dideoxy-D-glycero-α-D-galacto-2-nonulopyranosyl)onate (13). Partly purified compound **12** (2.1 g, 3.5 mmol) was stirred at room temperature in methanolic sodium methoxide (0.03 M, 180 mL) for 3 h. The solution was neutralized with 10% aqueous HCl and concentrated. Column chromatography (CH_2Cl_2/MeOH 20:1) afforded 927 mg of pure **13**[32] (65%). ^{1}H NMR (CD_3OD): δ 1.45 (s, 9H, −C(CH_3)$_3$), 1.70 (bt, 1H, J = 12.6 Hz, H3$_{ax}$), 2.63 (m, 1H, J_{H3ax} = 12.9 Hz, J_{H4} = 4.5 Hz, H3$_{eq}$), 3.33 (s, 3H, OCH_3), 3.43−3.66, 3.83−3.88 (2m, 7H, H4, H5, H6, H7, H8, H9$_a$, H9$_b$), 3.83 (s, 3H, COOCH_3).

Methyl (*O*-Methyl-5-(*N*-*tert*-butoxycarbonyl)-4,7,8,9-tetra-*O*-acetyl-3,5-dideoxy-D-glycero-α-D-galacto-2-nonulopyranosyl)onate (14). To a 0 °C solution of **13** (1.21 g, 3.1 mmol) in pyridine (100 mL), Ac_2O (60 mL) was added in small portions. The reaction mixture was stirred at room temperature overnight, concentrated, and coevaporated with toluene. Column chromatography (toluene/ethanol 8:1) afforded 1.56 g of **14** (92%). ^{1}H NMR ($CDCl_3$): δ 1.39 (s, 9H, (CH_3)$_3$), 1.84−1.95 (m, 1H, H3$_{ax}$), 2.03, 2.04, 2.13, 2.14 (4s, 3H each, 4Ac), 2.58 (dd, 1H, J_{H3ax} = 12.8 Hz, J_{H4} = 4.5 Hz, H3$_{eq}$), 3.31 (s, 3H, −OCH_3), 3.74−3.80 (m, 1H, H5), 3.80 (s, 3H, −COOCH_3), 4.0−4.14 (m, 2H, H6, H9$_a$), 4.18 (d, J_{H5} = 10.6 Hz, 1H, NH), 4.3 (d, J_{H8} = 11.53 Hz, 1H, H9$_b$), 4.7−4.8 (m, 1H, H4), 5.4−5.5 (m, 2H, H7, H8).

General Procedure for Preparation of Methyl (*O*-Methyl-5-*N*-acyl-4,7,8,9-tetra-*O*-acetyl-3,5-dideoxy-D-glycero-α-D-galacto-2-nonulopyranosyl)onates (16a−e). To a solution of **14** (0.38−0.40 mmol) in CH_2Cl_2 (6 mL), 90% aqueous TFA (2 mL) was added. The reaction mixture was stirred at room temperature for 1−2 h and monitored with TLC (toluene/acetone 1:1). The reaction mixture was concentrated, coevaporated with toluene, and dried extensively in vacuo to give the ammonium salt **15**. To a solution of **15** in dry CH_2Cl_2 (2 mL), RCOOH (1.2 equiv), HATU (1.2 equiv according to the acid), and DIPEA (3 eq, 0.2 mL) were added in the given order. The reaction mixture was stirred at room temperature under nitrogen and monitored by LCMS. After being stirred for 3−5 h, the reaction mixture was diluted with CH_2Cl_2, washed with water, saturated $NaHCO_3$, and water, dried, and concentrated. Column chromatography (toluene/ethanol 10:1) followed by preparative HPLC yielded **16a−e**.

Methyl (*O*-Methyl-5-*N*-propionyl-4,7,8,9-tetra-*O*-acetyl-3,5-dideoxy-D-glycero-α-D-galacto-2-nonulopyranosyl)onate (16a). Yield, 114 mg (56%). ^{1}H NMR ($CDCl_3$): δ 1.07 (t, 3H, CH_2CH_3), 1.94 (bt, 1H, J = 12.5 Hz, H3$_{ax}$), 2.00, 2.03, 2.13, 2.15 (4s, 3H each, 4Ac), 2.05−2.12 (m, 2H, CH_2CH_3), 2.56 (dd, 1H, J_{H3ax} = 12.9 Hz, J_{H4} = 4.7 Hz, H3$_{eq}$), 3.32 (s, 3H, OCH_3), 3.81 (s, 3H, COOCH_3), 4.05−4.16 (m, 3H, H5, H6, H9$_a$), 4.29 (dd, J_{H8} = 15.13 Hz, J_{H9a} = 2.7 Hz, 1H, H9$_b$), 4.80−4.93 (m, 1H, H4), 5.10 (d, J_{H5} = 9.3 Hz, 1H, NH), 5.3 (dd, J = 1.66 Hz, J = 10.13 Hz, 1H, H7), 5.38−5.46 (m, 1H, H8).

Methyl (*O*-Methyl-5-*N*-butanoyl-4,7,8,9-tetra-*O*-acetyl-3,5-dideoxy-D-glycero-α-D-galacto-2-nonulopyranosyl)onate (16b). Yield, 186 mg (92%). ^{1}H NMR ($CDCl_3$): δ 0.85, (t, J = 7.37 Hz, 3H, CH_3), 1.47−1.57 (m, 2H, CH_2CH_3), 1.87 (bt, 1H, J = 12.6, H3$_{ax}$), 1.95, 1.98, 2.08, 2.09 (4s, 3H each, 4Ac), 1.92−2.08 (m, 2H, CH_2CH_2−), 2.52 (dd, 1H, J_{H3ax} = 12.7 Hz, J_{H4} = 4.6 Hz, H3$_{eq}$), 3.26 (s, 3H, OCH_3), 3.75 (s, 3H, COOCH_3), 4.02−4.10 (m, 3H, H5, H6, H9$_a$), 4.25 (dd, J_{H8} = 12.40 Hz, J_{H9a} = 2.75 Hz, 1H, H9$_b$), 4.76−4.88 (m, 1H, H4), 5.26 (dd, J = 1.94 Hz, J = 8.31 Hz, 1H, H7), 5.34−5.39 (m, 2H, NH, H8).

Methyl (*O*-Methyl-5-*N*-isobutanoyl-4,7,8,9-tetra-*O*-acetyl-3,5-dideoxy-D-glycero-α-D-galacto-2-nonulopyranosyl)onate (16c). Yield, 65 mg (26%). ^{1}H NMR ($CDCl_3$): δ 1.02−1.1 (m, 6H, CH(CH_3)$_2$), 1.95 (bt, 1H, J = 12.7 Hz, H3$_{ax}$), 2.00, 2.03, 2.13, 2.15 (4s, 3H each, 4Ac), 2.21−2.32 (m, 1H, CH(CH$_3$)$_2$), 2.56 (dd, 1H, J_{H3ax} = 12.8 Hz, J_{H4} = 4.6 Hz, H3$_{eq}$), 3.32 (s, 3H, OCH_3), 3.81 (s, 3H, COOCH_3), 4.03−4.19 (m, 3H, H5, H6, H9$_a$), 4.31 (dd, J_{H8} = 12.44 Hz, J_{H9a} = 2.72 Hz, 1H, H9$_b$), 4.85−4.95 (m, 1H, H4), 5.25−5.35 (m, 2H, NH, H7), 5.37−5.44 (m, 1H, H8).

Methyl (*O*-Methyl-5-*N*-pentanoyl-4,7,8,9-tetra-*O*-acetyl-3,5-dideoxy-D-glycero-α-D-galacto-2-nonulopyranosyl)onate (16d). Yield, 137 mg (64%). ^{1}H NMR ($CDCl_3$): δ 0.85 (t, J_{CH2} = 7.32, 3H, CH_2CH_3), 1.23−1.37 (m, 2H, −CH_2CH_3), 1.45−1.59 (m, 2H, $CH_2CH_2CH_2$−), 1.93 (m, 1H, J = 12.6 Hz, H3$_{ax}$), 2.01, 2.04, 2.14, 2.15 (4s, 3H each, 4Ac), 2.04−2.14 (m, 2H, $CH_2CH_2CH_2$−), 2.57 (dd, 1H, J_{H3ax} = 12.9 Hz, J_{H4} = 4.6 Hz, H3$_{eq}$), 3.32 (s, 3H, OCH_3), 3.81 (s, 3H, COOCH_3), 3.99−4.18 (m, 3H, H5, H6, H9$_a$), 4.31 (dd, J_{H8} = 15.14 Hz, J_{H9a} = 4.31 Hz, 1H, H9$_b$), 4.84−4.94 (m, 1H, H4), 5.24−5.33 (m, 2H, NH, H7), 5.38−5.45 (m, 1H, H8).

Methyl (*O*-Methyl-5-*N*-benzoyl-4,7,8,9-tetra-*O*-acetyl-3,5-dideoxy-D-glycero-α-D-galacto-2-nonulopyranosyl)onate (16e). Yield, 89 mg (39%). ^{1}H NMR ($CDCl_3$): δ 1.95, 1.98, 2.13, 2.20 (4s, 3H each, 4Ac), 1.97−2.03 (m, 1H, H3$_{ax}$), 2.63 (dd, 1H, J_{H3ax} = 12.8 Hz, J_{H4} = 4.6 Hz, H3$_{eq}$), 3.34 (s, 3H, OCH_3), 3.79 (s, 3H, COOCH_3), 4.08 (dd, J_{H8} = 12.41 Hz, J_{H9a} = 5.82 Hz, 1H, H9$_b$), 4.23−4.33 (m, 3H, H5, H6, H9$_a$), 5.00−5.09 (m, 1H, H4), 5.30−5.35 (m, 1H, H7), 5.42−5.47 (m, 1H, H8), 5.93 (d, J_{H5} = 8.87, 1H, NH), 7.36−7.50 (m, 5H, Ar).

Methyl (*O*-Methyl-5-*N*-trifluoroacetamido-4,7,8,9-tetra-*O*-acetyl-3,5-dideoxy-D-glycero-α-D-galacto-2-nonulopyranosyl)onate (16f). To a solution of **14** (220 mg, 0.39 mmol) in CH_2Cl_2 (6 mL), 90% aqueous TFA (2 mL) was added. The reaction mixture was stirred at room temperature for 1 h and monitored with TLC (toluene/acetone 1:1). The reaction mixture was concentrated, coevaporated with toluene, and dried extensively in vacuo to give the ammonium salt **15**. To a solution of **15** in dry CH_2Cl_2 (4 mL) at 0 °C, trifluoroacetic anhydride (108 μL, 0.78 mmol, 2 equiv) and DMAP (95 mg, 0.78 mmol, 2 equiv) were added in the given order. The reaction mixture was stirred at room temperature under nitrogen and monitored by LCMS. After being stirred for 30 min, the reaction mixture was diluted with CH_2Cl_2, washed with water and saturated $NaHCO_3$ (aq) and water, dried, and concentrated. Repeated column chromatography (toluene/ethanol 10:1) gave 114 mg **16f** (56%). ^{1}H NMR ($CDCl_3$): δ 1.94 (bt, 1H, J = 12.6 Hz, H3$_{ax}$), 2.02, 2.04, 2.14, 2.17 (4s, 3H each, 4Ac), 2.62 (m, 1H, J_{H3ax} = 12.9 Hz, J_{H4} = 4.7 Hz H3$_{eq}$), 3.33 (s, 3H, OCH_3), 3.82 (s, 3H, COOCH_3), 3.93−4.05 (m, 1H, H5), 4.13 (dd, J_{H8} = 18.01 Hz, J_{H9a} = 5.50 Hz, 1H, H9$_b$), 4.26−4.37 (m, 2H, H6, H9$_a$), 4.94−5.05 (m, 1H, H4), 5.30 (dd, 1H, J = 2.08, J = 10.18, H7), 5.38−5.45 (m, 1H, H8), 6.52 (d, J_{H5} = 9.98, 1H, NH). ^{19}F NMR ($CDCl_3$): −76.7.

Methyl (*O*-Methy-5-*N*-methoxycarbonyl-4,7,8,9-tetra-*O*-acetyl-3,5-dideoxy-D-glycero-α-D-galacto-2-nonulopyranosyl)onate (16g). To a solution of **14** (201 mg, 0.36 mmol) in CH_2Cl_2 (6 mL), 90% aqueous TFA (2 mL) was added. The reaction mixture was stirred at room temperature for 1 h and monitored with TLC (toluene/acetone 1:1). The reaction mixture was concentrated, coevaporated with toluene, and dried extensively in vacuo to give the ammonium salt **15**. To a solution of **15** (0.26 mmol) in dry CH_2Cl_2 (3 mL), DIPEA was added (132 μL, 0.78 mmol, 3 equiv). The mixture was cooled to 0 °C before adding methyl chloroformate (60 μL, 0.78 mmol, 3 equiv) dropwise. The reaction mixture was stirred at room temperature under nitrogen, which was followed by LCMS. After being stirred for 1.5 h, the reaction mixture was diluted with CH_2Cl_2, washed with water, 1 M aqueous HCl, and water, dried, and concentrated. Column chromatography (toluene/acetone 4;1) afforded 90 mg of **16g** (66%). ^{1}H NMR ($CDCl_3$): δ 1.89 (bt, 1H, J = 12.6 Hz, H3$_{ax}$), 2.03, 2.04, 2.15, 2.15 (4s, 3H each, 4Ac), 2.61

(dd, 1H, J_{H3ax} = 12.8 Hz, J_{H4} = 4.6 Hz $H3_{eq}$), 3.32 (s, 3H, OCH_3), 3.62 (s, 3H, $NHCOOCH_3$), 3.67−3.78 (m, 1H, H5), 3.81 (s, 3H, $COOCH_3$), 4.05−4.15 (m, 2H, H6, $H9_a$), 4.30−4.35 (m, 1H, $H9_b$), 4.42 (d, J_{H5} = 9.76, 1H, NH), 4.79−4.90 (m, 1H, H4), 5.36−5.47 (m, 2H, H7, H8).

Methyl (*O*-Methyl-5-*N*-(3-methylureido)-4,7,8,9-tetra-*O*-acetyl-3,5-dideoxy-D-glycero-α-D-galacto-2-nonulopyranosyl)onate (16h). To a solution of **14** (100 mg, 0.18 mmol) in CH_2Cl_2 (3 mL), 90% aqueous TFA (1 mL) was added. The reaction mixture was stirred at room temperature for 1 h and monitored with TLC (toluene/acetone 1:1). The reaction mixture was concentrated, coevaporated with toluene, and dried extensively in vacuo to give the ammonium salt **15**. To a solution of **15** in dry CH_2Cl_2 (2 mL), DIPEA was added (125 μL, 0.72 mmol, 4 equiv). The mixture was cooled to 0 °C before methyl isocyanate was added dropwise (106 μL, 1.8 mmol, 10 equiv). The reaction mixture was stirred at room temperature under nitrogen, which was followed by LCMS. After being stirred for 4 h, the reaction mixture was diluted with CH_2Cl_2, washed with water, 1 M aqueous HCl, and water, dried, and concentrated. Column chromatography (toluene/ethanol 10:1) afforded 62 mg of **16h** (66%). ^{1}H NMR ($CDCl_3$): δ 1.95 (bt, 1H, *J* = 12.6 Hz, $H3_{ax}$), 2.027, 2.034, 2.14, 2.16 (4s, 3H each, 4Ac), 2.56 (dd, 1H, J_{H3ax} = 12.9 Hz, J_{H4} = 4.6 Hz $H3_{eq}$), 2.70 (s, 3H, $NHCH_3$), 3.33 (s, 3H, OCH_3), 3.81 (s, 3H, $COOCH_3$), 3.88−3.98 (m, 1H, H5), 4.03−4.22 (m, 3H, H6, $H9_a$, NH), 4.36 (dd, 1H, J_{H9a} = 12.5 Hz, J_{H8} = 2.4 Hz $H9_b$), 4.80−4.91 (m, 1H, H4), 5.35−5.47 (m, 2H, H7, H8).

General Procedure for Preparation of *O*-Methyl-5-*N*-acyl-3,5-dideoxy-D-glycero-α-D-galacto-2-nonulopyranosylonic Acids (17a−h). The *N*-acyl modified methylsialosides **16a−h** (0.10−0.30 mmol) were stirred in methanolic sodium methoxide (0.03 M, 7−15 mL) for 2 h. Complete O-deacetylation was confirmed with LCMS. The solutions were neutralized with Amberlite IR-120, filtered, and concentrated. The residues were diluted in methanol (4−8 mL), and LiOH (2 M (aq), 6 equiv) was added and stirred at room temperature overnight. The hydrolysis of the methyl esters was monitored by LCMS. The solutions were carefully neutralized with Amberlite IR-120, filtered, and concentrated. Purification by HPLC and lyophilization gave the products **17a−h**. Compounds **17a−e** and **17g**,**h** were estimated to be >95% pure according to hydrophilic interaction liquid chromatography (HILIC) and detection with MS (see Supporting Information for details). No UV-active impurities were observed with analytical reversed-phase HPLC and UV detection at 214 nm.

***O*-Methyl-5-*N*-propaonyl-3,5-dideoxy-D-glycero-α-D-galacto-2-nonulopyranosylonic Acid (17a).** Yield, 73 mg (100%). $[\alpha]_D^{20}$ 10 (*c* 0.67, MeOH). ^{1}H NMR (CD_3OD): δ 1.14 (t, J_{CH2} = 7.60 Hz, 3H, CH_2CH_3), 1.59−1.69 (m, 1H, $H3_{ax}$), 2.27 (q, J_{CH3} = 7.60, 2H, CH_2CH_3), 2.73 (dd, 1H, J_{H3ax} = 12.8 Hz, J_{H4} = 4.1 Hz $H3_{eq}$), 3.36 (s, 3H, OCH_3), 3.47−3.91 (m, 7H, H4, H5, H6, H7, H8, $H9_a$, $H9_b$). HRMS (FAB) calcd for $C_{13}H_{23}NO_9$: 382.1091 [M + 2Na − 2H]. Found: 382.1111.

***O*-Methyl-5-*N*-butanoyl-3,5-dideoxy-D-glycero-α-D-galacto-2-nonulopyranosylonic Acid (17b).** Yield, 92 mg (97%). $[\alpha]_D^{20}$ 8.9 (*c* 0.27, MeOH). ^{1}H NMR (CD_3OD): δ 0.96 (t, J_{CH2} = 7.40 Hz, 3H, CH_2CH_3), 1.61−1.70 (m, 3H, CH_2CH_3, $H3_{ax}$), 2.19−2.27 (m, 2H, $CH_2CH_2CH_3$), 2.74 (dd, 1H, J_{H3ax} = 12.8 Hz, J_{H4} = 4.1 Hz, $H3_{eq}$), 3.36 (s, 3H, OCH_3), 3.49−3.91 (m, 7H, H4, H5, H6, H7, H8, $H9_a$, $H9_b$). HRMS (FAB) calcd for $C_{14}H_{25}NO_9$: 396.1247 [M + 2Na − 2H]. Found: 396.1236.

***O*-Methyl-5-*N*-isobutanoyl-3,5-dideoxy-D-glycero-α-D-galacto-2-nonulopyranosylonic Acid (17c).** Yield, 28.4 mg (74%). $[\alpha]_D^{20}$ −16.5 (*c* 0.26, H_2O). ^{1}H NMR (CD_3OD): δ 1.10−1.17 (m, 6H, $CH(CH_3)_2$) 1.65−1.77 (m, 1H, $H3_{ax}$), 2.45−2.56 (m, 1H, $CH(CH_3)_2$), 2.70 (m, 1H, J_{H3ax} = 12.7 Hz, J_{H4} = 4.1 Hz, $H3_{eq}$), 3.37 (s, 3H, OCH_3), 3.46−3.91 (m, 7H, H4, H5, H6, H7, H8, $H9_a$, $H9_b$). HRMS (FAB) calcd for $C_{14}H_{25}NO_9$: 396.1247 [M + 2Na − 2H]. Found: 396.1251.

***O*-Methyl-5-*N*-pentanoyl-3,5-dideoxy-D-glycero-α-D-galacto-2-nonulopyranosylonic Acid (17d).** Yield, 68 mg (85%). $[\alpha]_D^{20}$ 7.7 (*c* 0.85, MeOH). ^{1}H NMR (CD_3OD): δ 0.96 (t, J_{CH2} = 7.32 Hz, 3H, CH_2CH_3), 1.33−1.45 (m, 2H, CH_2CH_3), 1.57−1.68 (m, 2H, $CH_2CH_2CH_3$), 1.68−1.78 (m, 1H, $H3_{ax}$), 2.21−2.31 (m, 2H, $COCH_2$-), 2.71 (dd, 1H, J_{H3ax} = 12.8 Hz, J_{H4} = 4.1 Hz, $H3_{eq}$), 3.39 (s, 3H, OCH_3), 3.53−3.91 (m, 7H, H4, H5, H6, H7, H8, $H9_a$, $H9_b$). HRMS (FAB) calcd for $C_{15}H_{27}NO_9$: 410.1404 [M + 2Na − 2H]. Found: 410.1399.

***O*-Methyl-5-*N*-benzoyl-3,5-dideoxy-D-glycero-α-D-galacto-2-nonulopyranosylonic Acid (17e).** Yield, 38 mg (78%). $[\alpha]_D^{20}$ 6.3 (*c* 0.83, MeOH). ^{1}H NMR (CD_3OD): δ 1.78 (bt, 1H, *J* = 12.2 Hz, $H3_{ax}$), 2.75 (dd, 1H, J_{H3ax} = 12.9 Hz, J_{H4} = 4.4 Hz $H3_{eq}$), 3.40 (s, 3H, $-OCH_3$), 3.56−4.07 (m, 7H, H4, H5, H6, H7, H8, $H9_a$, $H9_b$), 7.39−7.58 (m, 3H, Ar), 7.87−7.89 (m, 2H, Ar). HRMS (FAB) calcd for $C_{17}H_{23}NO_9$: 430.1091 [M + 2Na − 2H]. Found: 430.1095.

***O*-Methyl-5-*N*-methoxycarbonyl-3,5-dideoxy-D-glycero-α-D-galacto-2-nonulopyranosylonic Acid (17g).** Yield, 47 mg (100%). $[\alpha]_D^{20}$ −2.9 (*c* 0.58, MeOH). ^{1}H NMR (CD_3OD): δ 1.67 (bt, 1H, *J* = 12.2 Hz, $H3_{ax}$), 2.69 (dd, 1H, J_H = 4.5 Hz, J_{H3ax} = 12.69 Hz, $H3_{eq}$), 3.36 (s, 3H, OCH_3), 3.46−3.93 (m, 10H, H4, H5, H6, H7, H8, $H9_a$, $H9_b$, $NHCO_2CH_3$). HRMS (FAB) calcd for $C_{12}H_{21}NO_{10}$: 384.0883 [M + 2Na − 2H]. Found: 384.0882.

***O*-Methyl-5-*N*-(3-methylureido)-3,5-dideoxy-D-glycero-α-D-galacto-2-nonulopyranosylonic Acid (17h).** Yield, 65 mg (100%). $[\alpha]_D^{20}$ 10.2 (*c* 0.84, MeOH). ^{1}H NMR (CD_3OD): δ 1.67 (bt, 1H, *J* = 12.1 Hz, $H3_{ax}$), 2.60−2.81 (m, 4H, $H3_{eq}$, $NHCH_3$), 3.36 (s, 3H, OCH_3), 3.44−3.97 (m, 7H, H4, H5, H6, H7, H8, $H9_a$, $H9_b$). HRMS (FAB) calcd for $C_{12}H_{22}N_2O_9$: 361.1223 [M + Na − H]. Found: 361.1222.

***O*-Methyl-5-*N*-*tert*-butoxycarbonyl-3,5-dideoxy-D-glycero-α-D-galacto-2-nonulopyranosylonic Acid (18).** To a solution of **13** (28 mg, 0.071 mmol) in MeOH (2 mL), LiOH (0.2 mL, 2 M aq, 6 equiv) was added. The solution was stirred at room temperature overnight and then carefully neutralized with Amberlite IR-120, filtered, and concentrated at reduced pressure. Lyophilization afforded 27 mg of **18** (quant). Compound **18** was estimated to be >95% pure according to hydrophilic interaction liquid chromatography (HILIC) and detection with MS (see Supporting Information for details). No UV-active impurities were observed with analytical reversed-phase HPLC and UV detection at 214 nm. $[\alpha]_D^{20}$ 14.4 (*c* 0.32, MeOH). ^{1}H NMR (CD_3OD): δ 1.45 (s, 9H, $C(CH_3)_3$), 1.53−1.60 (m, 1H, $H3_{ax}$), 2.75−2.79 (m, 1H, $H3_{eq}$), 3.35 (s, 3H, OCH_3), 3.36−3.43 (m, 1H, H5), 3.53−3.65, 3.83−3.92 (2m, 6H, H4, H6, H7, H8, $H9_a$, $H9_b$), 6.75 (d, J_{H5} = 6.74 Hz, 1H, NH). HRMS (FAB) calcd for $C_{15}H_{27}NO_{10}$: 426.1353 [M + 2Na − 2H]. Found: 426.1353.

Methyl (5-Fmoc-aminopentyl[5-(*N*-*tert*-butoxycarbonylamido)-4,7,8,9-tetra-*O*-acetyl-3,5-dideoxy-D-glycero-α-D-galacto-2-nonulopyranosyl])onate (19). Compound **6** (50 mg, 0.078 mmol), Fmoc-aminopentanol (127 mg, 0.39 mmol), and powdered molecular sieves (3 Å, 0.17 g) were stirred in a mixture of CH_3CN and CH_2Cl_2 (3:2, 3 mL) for 1 h under nitrogen. Silver trifluoromethanesulfonate (40 mg, 0.16 mmol) was added, and the reaction mixture was cooled to −72 °C. Iodine monobromide in CH_2Cl_2 (0.5 M, 240 μL, 0.12 mmol) was added, and the mixture was stirred for 4 h. DIPEA (127 μL, 0.51 mmol) was added, and stirring was continued for 30 min. The mixture was allowed to come to room temperature before being filtered and concentrated in vacuo. Repeated column chromatography of the residue (silica gel, 30−70 μm, toluene/acetone, 4:1, petroleum ether/ethyl acetate, 1.5:1) afforded 46 mg of the title product **19** as a white powder (68%). $[\alpha]_D^{20}$ −7.5 (*c* 1.0, MeOH). ^{1}H NMR ($CDCl_3$): δ 1.39 (s, 9H, $C(CH_3)_3$, 2H, OCH_2-$CH_2CH_2CH_2CH_2NH$−), 1.51−1.60 (m, 4H, $OCH_2CH_2CH_2CH_2$-CH_2NH−), 1.91 (bt, 1H, *J* = 12.4 Hz, $H3_{ax}$), 2.02 (s, 6H, 2Ac), 2.13 (s, 3H, Ac), 2.14 (s, 3H, Ac), 2.58 (dd, 1H, J_{H3ax} = 12.4 Hz, J_{H4} = 4.4 Hz, $H3_{eq}$), 3.15−3.27 (m, 2H, OCH_2CH_2−, 1H, CH_2CH_2NH−), 3.72−3.81 (m, 2H, H5, CH_2CH_2NH−), 3.78 (s, 3H, CO_2CH_3), 3.99−4.10 (m, 2H, H6, H9a), 4.19 (d, 1H, J_{H5} = 10.4 Hz, CHN*H*), 4.21(t, 1H, J_{OCH2CH} = 6.8 Hz, OCH_2CH−), 4.33 (dd, 1H, J_{H8} = 2.4 Hz, J_{H9a} = 12.0 Hz, H9b), 4.39 (d, 2H, J_{OCH2CH} = 6.8 Hz, OCH_2CH−), 4.72−4.81 (m, 1H, H4), 5.12(bs, 1H, $-CH_2NH$), 5.37−5.46 (m, 2H, H7, H8).

General Procedure for Preparation of Methyl (5-Fmoc-aminopentyl[5-*N*-acyl-4,7,8,9-tetra-*O*-acetyl-3,5-dideoxy-D-glycero-α-galacto-2-nonylopyranosyl])onates (20a−c). To a solution of **19** (0.10−0.20 mmol) in CH_2Cl_2 (1.0−2.0 mL), 90% aqueous TFA (0.3−0.6 mL) was added. The reaction mixture was stirred at room temperature for 1 h, followed by TLC (toluene/acetone 2:1). When the Boc removal was complete, the mixtures were coevaporated with toluene and dried extensively in vacuo to give the corresponding ammonium salt. To a solution of the salt in dry CH_2Cl_2 (0.8−1.5 mL), RCOOH (1.2 equiv) and HATU (1.2 equiv according to the acid) and DIPEA (3.5 equiv) were added in the given order. The reaction was monitored by TLC (toluene/acetone 2:1) and LCMS, and after being stirred for 9−24 h at room temperature, the reaction mixture was diluted with CH_2Cl_2 and washed with 0.5 M aq HCl and water before being dried over Na_2SO_4. Repeated column chromatography (toluene/acetone; 2:1) of the residue afforded **20a−c**.

Methyl (5-Fmoc-aminopentyl[5-*N*-propanoyl-4,7,8,9-tetra-*O*-acetyl-3,5-dideoxy-D-glycero-α-galacto-2-nonylopyranosyl])-onate (20a). Yield, 53.0 mg (64%). $[\alpha]_D^{20}$ −9.8 (*c* 1.0, MeOH). ^{1}H NMR ($CDCl_3$): δ 1.08 (t, 3H, J_{CH2CH3} = 7.6 Hz, CH_2CH_3), 1.33−1.44 (m, 2H, $OCH_2CH_2CH_2CH_2CH_2NH$−), 1.48−1.59 (m, 4H, $OCH_2CH_2CH_2CH_2CH_2NH$−), 1.96 (bt, 1H, *J* = 12.8 Hz, $H3_{ax}$), 2.00 (s, 3H, Ac), 2.02 (s, 3H, Ac), 2.07 (q, 2H, J_{CH2CH3} = 7.6 Hz, CH_2CH_3), 2.13 (s, 3H, Ac), 2.15 (s, 3H, Ac), 2.57 (dd, 1H, J_{H3ax} = 12.8 Hz, J_{H4} = 4.8 Hz, $H3_{eq}$), 3.15−3.29 (m, 2H, OCH_2CH_2, 1H, CH_2CH_2NH), 3.71−3.81 (m, 1H, CH_2CH_2NH), 3.79 (s, 3H, CO_2CH_3), 4.02−4.14 (m, 3H, H5, H6, H9a), 4.25 (t, 1H, J_{OCH2CH} = 7.2 Hz, OCH_2CH), 4.34 (dd, 1H, J_{H8} = 2.4 Hz, J_{H9a} = 12.8 Hz, H9b), 4.39 (d, 2H, J_{OCH2CH} = 7.2 Hz, OCH_2CH), 4.81−4.90 (m, 1H, H4), 5.05−5.17 (m, 2H, NH), 5.29 (d, 1H, J_{H8} = 8.8 Hz, H7), 5.39−5.45 (m, 1H, H8).

Methyl (5-Fmoc-aminopentyl[5-*N*-butanoyl-4,7,8,9-tetra-*O*-acetyl-3,5-dideoxy-D-glycero-α-galacto-2-nonylopyranosyl])-onate (20b). Yield, 68 mg (66%). $[\alpha]_D^{20}$ −8.9 (*c* 1.0, MeOH). ^{1}H NMR ($CDCl_3$): δ 0.91 (t, 3H, J_{CH2CH3}= 7.2 Hz, CH_2CH_3), 1.32−1.45 (m, 2H, $OCH_2CH_2CH_2CH_2CH_2NH$), 1.49−1.61 (m, 6H, $OCH_2CH_2CH_2CH_2CH_2NH$, $CH_2CH_2CH_3$), 1.95 (bt, 1H, *J* = 12.8 Hz, $H3_{ax}$), 2.00 (s, 3H, Ac), 2.01 (s, 3H, Ac), 2.08 (t, 2H, J_{CH2CH2}= 7.6 Hz, CH_2CH_2), 2.14 (s, 3H, Ac), 2.14 (s, 3H, Ac), 2.58 (dd, 1H, J_{H3ax} = 12.8 Hz, J_{H4} = 4.4 Hz, $H3_{eq}$), 3.16−3.28 (m, 2H, OCH_2CH_2, 1H, CH_2CH_2NH), 3.73−3.82 (m, 1H, CH_2CH_2NH), 3.79 (s, 3H, CO_2CH_3), 4.01−4.06 (m, 1H, H9a), 4.08−4.13 (m, 2H, H5, H6), 4.21(t, 1H, J_{OCH2CH} = 6.8 Hz, OCH_2CH), 4.33 (dd, 1H, J_{H8} = 2.8 Hz, J_{H9a} = 12.0 Hz, H9b), 4.39 (d, 2H, J_{OCH2CH} = 6.8 Hz, OCH_2CH−), 4.81−4.91 (m, 1H, H4), 5.06−5.16 (m, 2H, N*H*), 5.28 (d, 1H, J_{H8} = 8.4 Hz, H7), 5.37−5.44 (m, 1H, H8).

Methyl (5-Fmoc-aminopentyl[5-*N*-isobutanoyl-4,7,8,9-tetra-*O*-acetyl-3,5-dideoxy-D-glycero-α-galacto-2-nonylopyranosyl])-onate (20c). Yield, 29 mg (18%). $[\alpha]_D^{20}$ −10.6 (*c* 1.0, MeOH). ^{1}H NMR ($CDCl_3$): δ 1.06 (d, 3H, $J_{CH(CH3)2}$ = 7.2 Hz, $CH(CH_3)_2$), 1.08 (d, 3H, $J_{CH(CH3)2}$ = 7.2 Hz, $CH(CH_3)_2$), 1.32−1.44 (m, 2H, $OCH_2CH_2CH_2CH_2CH_2NH$), 1.48−1.61 (m, 4H, $OCH_2CH_2CH_2CH_2CH_2NH$), 1.96 (bt, 1H, *J* = 12.0 Hz, $H3_{ax}$), 1.99 (s, 3H, Ac), 2.01 (s, 3H, Ac), 2.13 (s, 3H, Ac), 2.15 (s, 3H, Ac), 2.18−2.26 (m, 1H, $CH(CH_3)_2$), 2.57 (dd, 1H, J_{H3ax} = 12.0 Hz, J_{H4} = 4.8 Hz, $H3_{eq}$), 3.14−3.29 (m, 2H, OCH_2CH_2, 1H, CH_2CH_2NH), 3.72−3.78 (m, 1H, CH_2CH_2NH), 3.79 (s, 3H, CO_2CH_3), 4.01−4.08 (m, 1H, H9a), 4.09−4.14 (m, 2H, H5, H6), 4.21 (t, 1H, J_{OCH2CH} = 7.2 Hz, OCH_2CH-), 4.33 (dd, 1H, J_{H8} = 2.8 Hz, J_{H9a} = 12.4 Hz, H9b), 4.40 (d, 2H, J_{OCH2CH} = 7.2 Hz, OCH_2CH), 4.83−4.92 (m, 1H, H4), 5.08−5.16 (m, 2H, N*H*), 5.26 (d, 1H, J_{H8} = 8.4 Hz, H7), 5.34−5.43 (m, 1H, H8).

General Procedure for Preparation of 5-(2-Decyloxy-3,4-dioxocylobut-1-enyl)aminopenthyl-[5-*N*-acyl-3,5-dideoxy-D-glycero-α-D-galacto-2-nonulopyranosylonic Acids (21a−c). The compounds **20a−c** (0.06−0.07 mmol) were stirred in methanolic sodium methoxide (6 mL, 0.03 M) for 1 h. The solutions were neutralized with Amberlite IR-120 and concentrated under reduced pressure. The residues were dissolved in MeOH (5.0 mL) before LiOH (0.4 mL, 1 M) was added. The solutions were stirred at room temperature overnight, carefully neutralized with Amberlite IR-120, and concentrated. The fully deprotected compounds **4a−c** were used without further purification. The compounds were dissolved in DMF (3.5 mL), and didecyl squarate (0.16−0.18 mmol) and Et_3N (1.3 equiv according to **20a−c**) were added. After 11 h, the solutions were coevaporated with toluene and CH_2Cl_2. The residues were purified by column chromatography (methanol/ethyl acetate, 1:3 → 1:2) to give the title products **21a−c** as white powders. Compounds **21a−c** were >95% pure according to analytical reversed-phase HPLC with UV detection (see Supporting Information for details).

5-(2-Decyloxy-3,4-dioxocylobut-1-enyl)aminopenthyl-[5-*N*-propanoyl-3,5-dideoxy-D-glycero-α-D-galacto-2-nonulopyranosylonic Acid (21a). Yield, 31 mg (73%) containing 4% of the corresponding β-anomer. $[\alpha]_D^{20}$ 3.1 (*c* 1.0, MeOH). ^{1}H NMR (CD_3OD): δ 0.90 (t, 3H, J_{CH2CH3} = 6.8 Hz, CH_2CH_3), 1.14 (t, 3H, J_{CH2CH3} = 7.6 Hz, CH_2CH_3), 1.23−1.50 (m, 16H), 1.56−1.69 (m, 5H), 1.78−1.86 (m, 2H, $C(sp^2)OCH_2CH_2$), 2.28 (q, 2H, J_{CH2CH3} = 7.6 Hz, $-CH_2CH_3$), 2.83 (dd, 1H, J_{H4} = 4.0 Hz, J_{H3ax} = 12.0 Hz, $H3_{eq}$), 3.42 (t, 1H, *J* = 6.8 Hz), 3.45−3.53 (m, 2H), 3.55−3.65 (m, 3H), 3.66−3.74 (m, 2H), 3.77−3.90 (m, 3H), 4.65−4.74 (m, 2H). HRMS (FAB) calcd for $C_{31}H_{52}N_2O_{12}$: 689.3239 [M + 2Na − 2H]. Found: 689.3222.

5-(2-Decyloxy-3,4-dioxocylobut-1-enyl)aminopenthyl-[5-*N*-butanoyl-3,5-dideoxy-D-glycero-α-D-galacto-2-nonulopyranosylonic Acid (21b). Yield, 23 mg (61%) containing 2% of the corresponding β-anomer. $[\alpha]_D^{20}$ 3.2 (*c* 1.0, MeOH). ^{1}H NMR (CD_3OD): δ 0.90 (t, 3H, J_{CH2CH3} = 6.8 Hz, CH_2CH_3), 0.96 (t, 3H, J_{CH2CH3} = 7.6 Hz, $-CH_2CH_3$), 1.27−1.50 (m, 16H), 1.53−1.71 (m, 7H), 1.80−1.90 (m, 2H, $C(sp^2)OCH_2CH_2$), 2.25 (t, 2H, J_{CH2CH2} = 6.8 Hz, CH_2CH_2), 2.83 (dd, 1H, J_{H3ax} = 12.0 Hz, J_{H4} = 4.8 Hz, $H3_{eq}$), 3.42 (t, 1H, *J* = 7.2 Hz), 3.46−3.53 (m, 2H), 3.55−3.65 (m, 3H), 3.66−3.75 (m, 2H), 3.76−3.92 (m, 3H), 4.64−4.75 (m, 2H). HRMS (FAB) calcd for $C_{32}H_{54}N_2O_{12}$: 703.3395 [M + 2Na − 2H]. Found: 703.3395.

5-(2-Decyloxy-3,4-dioxocylobut-1-enyl)aminopenthyl-[5-*N*-isobutanoyl-3,5-dideoxy-D-glycero-α-D-galacto-2-nonulopyranosylonic Acid (21c). Yield, 31 mg (80%). $[\alpha]_D^{20}$ 4.7 (*c* 1.0, MeOH). ^{1}H NMR (CD_3OD): δ 0.90 (t, 3H, J_{CH2CH3} = 6.8 Hz, CH_2CH_3), 1.13 (d, 6H, $J_{CH(CH3)2}$ = 6.8 Hz, $-CH(CH_3)_2$), 1.25−1.50 (m, 16H), 1.52−1.71 (m, 5H), 1.75−1.89 (m, 2H, $C(sp^2)OCH_2CH_2$), 2.53 (sep, 1H, $J_{CH(CH3)2}$ = 6.8 Hz, $CH(CH_3)_2$), 2.83 (dd, 1H, J_{H4} = 4.8 Hz, J_{H3ax} = 16.4 Hz, $H3_{eq}$), 3.38−3.53 (m, 3H), 3.54−3.77 (m, 5H), 3.77−3.95 (m, 3H), 4.65−4.76 (m, 2H). HRMS (FAB) calcd for $C_{32}H_{54}N_2O_{12}$: 703.3395 [M + 2Na − 2H]. Found: 703.3401.

Conjugation of 21a−c to HSA. Each of the compounds **21a−c** (14.5 mg, 0.0225 mmol) was added to HSA (25 mg, 0.38 μmol) in 1.0 mL of $NaHCO_3$ buffer (pH 9.1). The mixtures were stirred at room temperature for 27 h, dialyzed against water (3 × 1000 mL) for 24 h, and lyophilized. The glycoproteins **22a−c** were obtained as white powders with 14, 17, and 16 saccharides per protein according to MALDI TOF MS and as confirmed by gel electrophoresis.

Acknowledgment. This work was supported by the Swedish Research Council, the J. C. Kempe Foundation, and the Jeansson Foundation. We thank Jan Kihlberg for valuable support throughout the project. Gunnar Grönberg of AstraZeneca R&D, Mölndal, Sweden, is gratefully acknowledged for help with structure determination of the degraded sialic acids **9a**,**b**. We are grateful to Anna Linusson and David Andersson for their support in computational chemistry. We thank Yvonne Nygren for valuable help with HPLC−MS analysis.

Supporting Information Available: General chemical methods and materials; experimental procedures and data for compounds **2a−e**, **7a**,**b**, **3a**,**b**, and **10a−i**; ^{13}C NMR data for compounds **13**, **14**, **16a−h**, **17a−h**, **18**, **19**, **20a−c**, and **21a−c**; experimental procedures for the binding and infectivity assays. This material is available free of charge via the Internet at http://pubs.acs.org.

References

(1) Flint, S. J.; Enquist, L. W.; Racaniello, V. R.; Skalka, A. M. *Principles of Virology*, 2nd ed.; ASM Press: Washington, D.C., 2004.
(2) Uhnoo, I. Antivirala läkemedels möjligheter och begränsningar. *Tidskr. Medikament* **2002**, *2*, 24–29.
(3) Jones, P. S. Strategies for antiviral drug discovery. *Antiviral Chem. Chemother.* **1998**, *9*, 283–302.
(4) De Clercq, E. Strategies in the design of antiviral drugs. *Nat. Rev. Drug Discovery* **2002**, *1*, 13–25.
(5) Mammen, M.; Choi, S. K.; Whitesides, G. M. Polyvalent interactions in biological systems: Implications for design and use of multivalent ligands and inhibitors. *Angew. Chem., Int. Ed.* **1998**, *37*, 2755–2794.
(6) Kiessling, L. L.; Pohl, N. L. Strength in numbers: Non-natural polyvalent carbohydrate derivatives. *Chem. Biol.* **1996**, *3*, 71–77.
(7) Borman, S. Multivalency: Strength in numbers. *Chem. Eng. News* **2000**, *78*, 48–53.
(8) Ford, E.; Nelson, K. E.; Warren, D. Epidemiology of epidemic keratoconjunctivitis. *Epidemiol. Rev.* **1987**, *9*, 244–261.
(9) Gordon, Y. J.; Aoki, K.; Kinchington, P. R. Adenovirus Keratoconjunctivitis. In *Ocular Infection and Immunity*; Pepose, J. S., Holland, G. N., Wilhelmus, K. R., Eds.; C.V. Mosby: St. Louis, MO, 1996.
(10) Aoki, K.; Kawana, R.; Matsumoto, I.; Wadell, G.; Dejong, J. C. Viral conjunctivitis with special reference to adenovirus type-37 and enterovirus-70 infection. *Jpn. J. Ophthalmol.* **1986**, *30*, 158–164.
(11) Paparello, S. F.; Rickman, L. S.; Mesbahi, H. N.; Ward, J. B.; Siojo, L. G.; et al. Epidemic keratoconjunctivitis at a United-States military base—Republic of the Philippines. *Mil. Med.* **1991**, *156*, 256–259.
(12) Kemp, M. C.; Hierholzer, J. C.; Cabradilla, C. P.; Obijeski, J. F. The changing etiology of epidemic keratokonjunctivitis: Antigenic and restriction enzyme analyses of adenovirus types 19 and 37 isolated over a 10-year period. *J. Infect. Dis.* **1983**, *148*, 24–33.
(13) Aoki, K.; Yoshitugu, T. A twenty-one year surveillance of adenoviral conjunctivitis in sapporo, japan. *Int. Ophthamol. Clin.* **2002**, *42*, 49–54.
(14) Henry, L. J.; Xia, D.; Wilke, M. E.; Deisenhofer, J.; Gerhard, R. D. Characterisation of the knob domain of the adenovirustype 5 fiber protein expressed in *Escherichia coli*. *J. Virol.* **1994**, *68*, 5239–5246.
(15) Arnberg, N.; Edlund, K.; Kidd, A. H.; Wadell, G. Adenovirus type 37 uses sialic acid as a cellular receptor. *J. Virol.* **2000**, *74*, 42–48.
(16) Arnberg, N.; Kidd, A. H.; Edlund, K.; Olfat, F.; Wadell, G. Initial interactions of subgenus D adenoviruses with A549 cellular receptors: Sialic acid versus alpha(v) integrins. *J. Virol* **2000**, *74*, 7691–7693.
(17) Kiessling, L. L.; Gestwicki, J. E.; Strong, L. E. Synthetic multivalent ligands in the exploration of cell−surface interactions. *Curr. Opin. Chem. Biol.* **2000**, *4*, 696–703.
(18) Johansson, S. M. C.; Arnberg, N.; Elofsson, M.; Wadell, G.; Kihlberg, J. Multivalent HSA conjugates of 3′-siallyllactose are potent inhibitors of adenoviral cell attachment and infection. *ChemBioChem* **2005**, *6*, 358–364.
(19) Johansson, S. M. C.; Nilsson, E. C.; Elofsson, M.; Ahlskog, N.; Kihlberg, J.; et al. Multivalent sialic acid conjugates inhibit adenovirus type 37 from binding to and infecting human corneal epithelial cells. *Antiviral Res.* **2007**, *73*, 92–100.
(20) Tietze, L. F.; Arlt, M.; Beller, M.; Glusenkamp, K. H.; Jahde, E.; et al. Anticancer agents. 15. Squaric acid diethyl ester, a new coupling reagent for the formation of drug biopolymer conjugates—synthesis of squaric acid ester amides and diamides. *Chem. Ber.* **1991**, *124*, 1215–1221.
(21) Tietze, L. F.; Schroter, C.; Gabius, S.; Brinck, U.; Goerlachgraw, A.; et al. Conjugation of para-aminophenyl glycosides with squaric acid diester to a carrier protein and the use of neoglycoprotein in the histochemical detection of lectins. *Bioconjugate Chem.* **1991**, *2*, 148–153.
(22) Bergh, A.; Magnusson, B. G.; Ohlsson, J.; Wellmar, U.; Nilsson, U. J. Didecyl squarate, a practical amino-reactive cross-linking reagent for neoglycoconjugate synthesis. *Glycoconjugate J.* **2001**, *18*, 615–621.
(23) Burmeister, W. P.; Guilligay, D.; Cusack, S.; Wadell, G.; Arnberg, N. Crystal structure of species D adenovirus fiber knobs and their sialic acid binding sites. *J. Virol.* **2004**, *78*, 7727–7736.
(24) Taylor, R. D.; Jewsbury, P. J.; Essex, J. W. A review of protein−small molecule docking methods. *J. Comput.-Aided Mol. Des.* **2002**, *16*, 151–166.
(25) Verdonk, M. L.; Cole, J. C.; Hartshorn, M. J.; Murray, C. W.; Taylor, R. D. Improved protein−ligand docking using gold. *Proteins: Struct., Funct., Genet.* **2003**, *52*, 609–623.
(26) Gohlke, H.; Klebe, G. Approaches to the description and prediction of the binding affinity of small-molecule ligands to macromolecular receptors. *Angew. Chem., Int. Ed.* **2002**, *41*, 2645–2676.
(27) Marra, A.; Sinay, P. Stereoselective synthesis of 2-thioglycosides of *N*-acetylneuraminic acid. *Carbohydr. Res.* **1989**, *187*, 35–42.
(28) Waglund, T.; Claesson, A. Stereoselective synthesis of the alpha-allyl C-glycoside of 3-deoxy-D-manno-2-octulosonic acid (KDO) by use of radical chemistry. *Acta Chem. Scand.* **1992**, *46*, 73–76.
(29) Sherman, A. A.; Yudina, O. N.; Shashkov, A. S.; Menshov, V. M.; Nifantiev, N. E. Preparative route to *N*-glycolylneuraminic acid phenyl 2-thioglycoside donor and synthesis of Neu5Gc-alpha-(2 → 3′)-lactosamine 3-aminopropyl glycoside. *Carbohydr. Res.* **2002**, *337*, 451–457.
(30) Saito, K.; Sugai, K.; Fujikura, K.; Yamada, N.; Goto, M.; et al. Thermal-degradation of sodium *N*-acetylneuraminate. *Carbohydr. Res.* **1989**, *185*, 307–314.
(31) Byramova, N. E.; Tuzikov, A. B.; Bovin, N. V. Studies on the synthesis of sialosides and sialic-acid analogs. 2. A simple procedure for the synthesis of the methyl and benzyl glycosides of Neu5Ac and 4-epi-Neu5Ac—conversion of the benzyl and methyl glycosides of Neu5Ac into *N*-trifluoroacetylneuraminic acid benzyl glycosides. *Carbohydr. Res.* **1992**, *237*, 161–175.
(32) Hori, H.; Nakajima, T.; Nishida, Y.; Ohrui, H.; Meguro, H. A simple method to determine the anomeric configuration of sialic-acid and its derivatives by C^{13}-NMR. *Tetrahedron Lett.* **1988**, *29*, 6317–6320.
(33) Mei, Y. F.; Lindman, K.; Wadell, G. Two closely related adenovirus genome types with kidney or respiratory tropism differ in their binding to epithelial cells of various origins. *Virology* **1998**, *240*, 254–266.
(34) Segerman, A.; Arnberg, N.; Eriksson, A.; Lindman, K.; Wadell, G. There are two different species B adenovirus receptors: sBAR, common to species BB and B2 adenoviruses, and SB2AR, excusively used by species B2 adenoviruses. *J. Virol.* **2003**, *77*, 1157–1162.
(35) Wadell, G.; Allard, A.; Hierholzer, J. C. *Manual of Clinical Microbiology*; ASM Press: Washington, DC, 1999; 970−982.
(36) *Reduce 2.21 for Linux*; The Richardson Laboratory, Duke University: Durham, NC; http://kinemage.biochem.duke.edu (accessed Feb 2005).
(37) *CS Chemdraw Ultra*, version 7.0.1 for Macintoch; CambridgeSoft Corp.: Cambridge, MA, 2002.
(38) Weininger, D. SMILES, a chemical language and information-system. 1. Introduction to methodology and encoding rules. *J. Chem. Inf. Comput. Sci.* **1988**, *28*, 31–36.
(39) *CORINA*; Molecular Networks GmbH: Erlangen, Germany; http://www2.chemie.uni-erlangen.de/sofware/corina/free_struct.html (accessed Feb 2005).
(40) *GOLD*, version 3.1.1; The Cambridge Crystallographic Data Center: Cambridge, U.K., 2004.
(41) *MOE—Molecular Operating Environment*, version 2004.03; Chemical Computing Group Inc.: Montreal, Canada, 2004.
(42) *SYBYL*, version 7.2; Tripos Inc.: St. Louis, MO, 2004.
(43) Jones, G.; Willett, P.; Glen, R. C. Molecular recognition of receptor-sites using a genetic algorithm with a description of desolvation. *J. Mol. Biol.* **1995**, *245*, 43–53.
(44) Jones, G.; Willett, P.; Glen, R. C.; Leach, A. R.; Taylor, R. Development and validation of a genetic algorithm for flexible docking. *J. Mol. Biol.* **1997**, *267*, 727–748.
(45) Rhodes, G. *Crystallography Made Crystal Clear*, 2nd ed.; Academic Press: San Diego, CA, 2000.

JM801609S